

1950

~~CONFIDENTIAL~~

2.2
Copy
RM E50F16
6

NACA RM E50F16

~~NACA~~

RESEARCH MEMORANDUM

ALTITUDE-TEST-CHAMBER INVESTIGATION OF PERFORMANCE
OF A 28-INCH RAM-JET ENGINE

I - COMBUSTION AND OPERATIONAL PERFORMANCE
OF FOUR COMBUSTION-CHAMBER CONFIGURATIONS

By W. L. Jones, T. B. Shillito
and J. G. Henzel, Jr.

Lewis Flight Propulsion Laboratory

CLASSIFICATION CHANGED
Cleveland, Ohio

UNCLASSIFIED

CLASSIFIED DOCUMENT

To

By authority of

NACA Research

RN-127

AMT 6-13-58

THIS DOCUMENT CONTAINS CLASSIFIED INFORMATION
affecting the National Defense of the United
States within the meaning of the Espionage Act,
UNC 50-31 and 50-32. Its transmission or the
revelation of its contents in any manner to an
unauthorized person is prohibited by law.
Information so classified may be imparted
only to persons in the military and naval
services of the United States, appropriate
civilian officers and employees of the Federal
Government who have a legitimate interest
therein, and to United States citizens of known
loyalty and discretion who of necessity must be
informed thereof.

*effective
May 16, 1958*

NATIONAL ADVISORY COMMITTEE FOR AERONAUTICS

WASHINGTON
August 23, 1950

~~CONFIDENTIAL~~



NATIONAL ADVISORY COMMITTEE FOR AERONAUTICS

RESEARCH MEMORANDUM

ALTITUDE-TEST-CHAMBER INVESTIGATION OF PERFORMANCE

OF A 28-INCH RAM-JET ENGINE

I - COMBUSTION AND OPERATIONAL PERFORMANCE

OF FOUR COMBUSTION-CHAMBER CONFIGURATIONS

By W. L. Jones, T. B. Shillito
and J. G. Henzel, Jr.

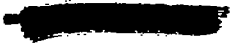
SUMMARY

An altitude-test-chamber investigation of a 28-inch-diameter ram-jet engine at a simulated flight Mach number of approximately 2.0 for altitudes of 40,000 to 50,000 feet was conducted at the NACA Lewis laboratory. Four configurations involving three different flame holders, varying in the number and size of the annular gutters, in conjunction with several fuel-injection systems were investigated.

One of the flame-holder fuel-system combinations investigated permitted smooth operation over a range of fuel-air ratios from 0.031 to 0.075 for the altitude range investigated. The combustion efficiency increased from 0.53 to over 0.9 with an increase in fuel-air ratio for these conditions. With this configuration, the performance of the engine approximated the original design requirements for satisfactory performance of the proposed flight vehicle in both climb and cruise.

INTRODUCTION

An altitude-test-chamber investigation of the altitude performance of a 28-inch-diameter ram-jet engine is being conducted at the NACA Lewis laboratory. This engine is being developed by the Marquardt Aircraft Company for use in a Grumman Aircraft



Engineering Corporation test vehicle as part of a Navy guided-missile program. The missile is intended to be launched by a rocket booster and is to climb under its own power to a cruising altitude of 50,000 feet. The anticipated flight speed during the climb and at cruising conditions is at a Mach number of 2.0.

The manufacturer is currently subjecting the engine to extensive direct connected developmental tests at various simulated altitudes from sea level to approximately 30,000 feet.

The performance investigation was extended to simulated altitudes of 50,000 feet at the Lewis laboratory and modifications were made to permit the attainment of the desired performance. The altitude operational limits, the temperature rise, and the combustion efficiency for altitudes from 40,000 to 50,000 feet are presented for four different combustion-chamber configurations with several fuel-injection systems. Typical cold-flow-pressure surveys and the combustion-chamber pressures and Mach numbers under burning conditions are also presented.

APPARATUS

Description of Engine

A schematic drawing of the test engine is shown in figure 1. The internal design of the test engine is similar to that of the flight engine with the exception of the installation of a bell-mouthed, convergent-divergent nozzle at the engine inlet. This nozzle was used in addition to the supersonic inlet diffuser of the flight engine (which is formed by a 20° cone and the forward edge or lip of the outer shell at station 100) in order to accelerate the air from stagnation conditions in the altitude test chamber to a Mach number of 1.6 at a position corresponding to the lip of the flight engine (station 100). The Mach number of 1.6 at the lip position corresponds to the lip Mach number of the flight engine at a flight Mach number of 2.0. This inlet-nozzle arrangement therefore permits simulation of the Mach number, pressure, and temperature conditions that occur downstream of the lip with the free-stream inlet of the flight configuration and serves to position the normal shock in the subsonic diffuser at the same location it would assume in flight, subject to limitations that will be subsequently discussed. Exact boundary-layer and air-flow

spill-over conditions of flight were not reproduced by this inlet configuration, however, so that the stability of the combustion-chamber and diffuser combination could not be investigated; moreover, possible effects of the inlet boundary layer on velocity and pressure distribution could not be evaluated.

From the lip station (station 100) to the end of the inner body, the annular air-flow passage formed by the inner body and the outer shell was divergent and had the same dimensions as the flight engine. This annular divergent passage was 209.36 inches long and had an area ratio of 4.3. The combustion chamber was circular in cross section with a diameter of 28 inches and a length of 46 inches and was followed by a convergent-divergent exit nozzle 19 inches long that had a throat diameter of 20.75 inches and an outlet diameter of 22.44 inches. The entire outer surface of the combustion chamber and exit nozzle was water-jacketed to provide cooling. Fuel was injected slightly downstream of station 266 and the flame holders were mounted near station 297. The fuel systems and flame holders are subsequently described in detail. The inner body was connected to the outer shell by four longerons that extended nearly the entire length of the inner body.

Installation in Altitude Test Chamber

The installation of the engine in the 10-foot-diameter altitude test chamber is shown in figure 2; details of the construction of the altitude test chamber are given in reference 1. The engine was mounted on a free-moving thrust platform that was connected to a calibrated air-balancing thrust cell. A diaphragm seal was fitted to the engine at a front baffle and provided an air-tight seal separating the inlet ram-pressure air from the altitude exhaust, thus permitting a pressure difference to be maintained across the engine. The rear baffle wall was installed to keep the hot exhaust gases from recirculating around the engine.

A sudden-expansion jet diffuser, similar in principle to the device described in reference 2, was installed at the exit of the engine. This jet diffuser was necessary to increase the high-altitude operational limits imposed by the laboratory altitude exhaust system. A sliding seal was placed around the engine at the entrance to the jet diffuser to minimize the air leakage into the diffuser.

Instrumentation

The fuel flow was measured with a calibrated orifice meter and the air flow was measured with a flat-plate orifice located in the supply line upstream of the test chamber. The locations of temperature and static- and total-pressure measurements within the engine are shown in figure 1. The engine-inlet total temperature and pressure were measured by thermocouple and pressure rakes at the bellmouth entrance. Total- and static-pressure surveys across the annular diffuser were made at the three locations shown in figure 1. Static pressures were also measured along the wall of the inner body. Water-cooled rakes were used to measure total pressures at the combustion-chamber outlet. Static pressure in the exhaust-nozzle throat was measured by wall static tubes and by water-cooled, trailing static tubes (having a length-diameter ratio of 27) mounted in the combustion chamber and extending downstream to the nozzle throat. Total pressure at the nozzle exit was measured by a water-cooled tail rake extending across the nozzle discharge.

Flame-Holder and Fuel-Injection Systems

A sketch of the fuel-injection system and flame-holder arrangement is presented in figure 3. Two different fuel-manifold systems were used, a single-manifold system and a double-manifold system. The single-manifold system was formed by the forward (upstream) manifold shown, and incorporated fuel nozzles spraying both upstream and downstream. This manifold was divided into two internal compartments in order to permit independent control of the fuel flow to the upstream and downstream fuel nozzles. The double-manifold system was formed by two manifolds at the locations illustrated. For this system, only upstream fuel nozzles were installed in both manifolds. Each fuel manifold was divided into four quadrants because of the presence of the longeron supports for the inner body (fig. 3). The fuel manifolds of the double-manifold system were adjustable in the radial direction, but were fixed in the longitudinal direction by structural considerations. The flame holders were mounted in the location shown in figure 3.

The following table summarizes the essential features of the flame-holder and fuel-injection systems used for the various ram-jet-engine configurations investigated:

Config- uration	Flame holder			Fuel-injection system			
	Blocked area (percent)	Gutter width (in.)	Number of gutters	Manifold system	Fuel nozzles	Diametrical location of fuel manifolds (in.)	
						Up- stream	Down- stream
1	42	1	4	Single	Flat- spray	24.6	--
2	42	1	4	Double	Spring- loaded	20.0	24.6
2	42	1	4	--Do.--	--Do.--	21.0	23.6
3	55	1	6	--Do.--	--Do.--	20.0	24.6
4	45	2	2	--Do.--	--Do.--	20.0	24.6

Configuration 1. - The single-manifold fuel system was used for configuration 1. Flat-spray, commercially available fuel nozzles of the type illustrated in figure 4 were installed in this manifold. These fuel nozzles provided a flat, fan-shaped spray in still air and were arranged so that 24 nozzles (with a combined capacity of 48 gal/min at a pressure of 100 lb/sq in.) sprayed upstream with the fan directed radially, and 12 nozzles (with a combined capacity of 22.5 gal/min) sprayed downstream with the fan directed tangentially. The 12 downstream nozzles were located in line with alternate upstream nozzles. The manifold segments were located at a diameter of 24.6 inches.

The flame holder used for this configuration (fig. 5) consisted of four V-type gutters, 1 inch wide at the open end, in annular rings supported by radial struts. The gutters were arranged in a staggered V in the longitudinal plane. The flare cases on the flame holder are for ignition in the flight configuration. For this investigation, ignition was provided by a spark plug installed in the igniter box shown in figure 5. A separate small quantity of fuel was supplied to this box (which is in reality a miniature ram jet) for the starting period and was shut off during the runs. The spark plug, which was inserted through the side of the igniter box, was of conventional construction. The total projected area of the flame holder, flare cases, and igniter box was 42 percent of the cross-sectional area of the combustion

chamber. This quantity will be hereinafter called the percentage of blocked area of the flame holder. Investigations with this configuration were conducted with and without the flare cases installed.

Configuration 2. - Configuration 2 and all subsequent configurations described used the double-manifold system and spring-loaded fuel nozzles of the type shown in figure 6 with 16 nozzles in the upstream manifold and 24 in the downstream manifold. These spring-loaded fuel nozzles, which were designed for the purpose of improving the spray characteristics at low fuel pressures, provided a hollow cone spray and incorporated a variable-area orifice having approximately linear flow against pressure characteristics that are described. During the investigation of this configuration, two diametrical positions of the fuel manifolds were used as indicated in the preceding table. The flame holder used was the same as used for configuration 1 (fig. 5).

Configuration 3. - The radial position of the fuel manifolds for this configuration was the same as the first position used for configuration 2. The flame holder used for configuration 3 had six annular-V gutters, each 1 inch wide, with V-shaped tabs (fig. 7) attached to the radial struts, resulting in a blocked area of 55 percent.

Configuration 4. - Configuration 4 had the same fuel system as configuration 3. The flame holder (fig. 8) had two annular-V gutters, each 2 inches wide at the open end. This flame holder also included flare cases and an igniter box and had a blocked area of 45 percent.

PROCEDURE

In order to satisfy the proposed flight plan, it will be necessary to maintain stable operation at fuel-air ratios from approximately 0.03 to 0.065 with combustion efficiencies varying in a uniform manner from 0.70 at a fuel-air ratio of 0.03 to 0.90 at a fuel-air ratio of 0.065 at an altitude of 50,000 feet and a flight Mach number of 2.0.

The preliminary phase of this investigation was conducted to determine the combustion efficiencies and the altitude blow-out limits at altitudes up to 50,000 feet and simulated flight Mach number of 2.0. The general procedure for most of the runs was to ignite the burner at bellmouth-inlet pressure of about 40 inches

of mercury absolute, temperature of 250° F, and engine-outlet pressure of 25 inches of mercury absolute with a fuel-air ratio of approximately 0.04. When stable burning was established, the exit pressure was slowly reduced until choking conditions were reached in the exit nozzle. The inlet and outlet pressures were then set to simulate the desired flight conditions. With these pressures held constant, the fuel-air ratio was varied in small intervals and data were taken at various stabilized burning conditions until rich or lean blow-out occurred. Runs were made with the various configurations at a simulated Mach number of 2.0 (inlet temperature, 250° F) at altitudes from 40,000 to 50,000 feet; additional data for configuration 1 were also taken at 37,000 feet.

For the single-manifold fuel system, all runs were made with equal fuel pressures applied to all nozzles. For the double-manifold fuel system, three different methods of injection were used:

1. Uniform injection: Equal fuel pressures to all nozzles in both upstream and downstream manifolds
2. Quadrant injection: Equal fuel pressures to nozzles in both upstream- and downstream-manifold segments in two diametrically opposite quadrants
3. Annular injection: Equal fuel pressures to all nozzles in either upstream or downstream manifold

Quadrant or annular injection was used to extend the operating range to leaner fuel-air ratios than were possible with uniform injection. The fuel used was commercial grade normal heptane.

Blow-out was detected by the change in sound level and by observation of the flame through periscopes so arranged as to view the discharge of the engine from the side and from a point directly downstream of the discharge. Photographs of the flame were taken through the downstream periscope.

In addition to the burning tests, a few cold-flow runs were also made. For these runs, a variable-area orifice was attached to the engine outlet and the pressure ratio across the engine was varied. Pressure distributions throughout the engine were measured for various engine-pressure ratios and outlet-orifice areas (corresponding to a range of combustion-chamber-inlet Mach numbers from 0.128 to 0.313).

1282

The symbols and station locations used throughout the report are defined in appendix A. Combustion temperatures and efficiencies were calculated by the methods outlined in appendix B.

COLD-FLOW PRESSURE-SURVEY RESULTS

The results of static-pressure surveys obtained with configuration 1 without burning are shown in figure 9(a). The ratio of the wall static pressure to the total pressure at the inlet to the bellmouth nozzle is plotted against the distance along the engine (or station, fig. 1). Lines are shown for various combustion-chamber-inlet Mach numbers from 0.13 to 0.30. It was impossible to determine these Mach numbers from direct measurement of the total and static pressures at the combustion-chamber inlet because of the presence of the flame holder immediately downstream of the inner body. Accordingly, measurements of total and static pressures at station 297 were used and the Mach number determined at that station was adjusted to the full combustion-chamber area. Although these Mach numbers may therefore be somewhat inaccurate, they are considered valid for reference purposes.

Although the Mach number and pressure relations illustrated were obtained over a range of simulated altitudes, they are substantially independent of this variable. In the convergent portion of the inlet nozzle, the air expands to sonic velocity with an attendant reduction in the static pressure. The channel downstream of the nozzle throat is constantly increasing in area up to the combustion-chamber inlet and, consequently, a further reduction in pressure, accompanied by an increase in Mach number, occurs downstream of the minimum area. Because the mass flow for a given inlet pressure and temperature is fixed by the choked flow at the inlet-nozzle throat, an adjustment in pressure is necessary somewhere in the divergent channel in order to satisfy continuity between the engine inlet and the combustion chamber. This adjustment takes place between the inlet-nozzle throat and the combustion-chamber inlet through the action of one or more shock waves. The presence of these shock waves is evidenced by the rapid increase in static wall pressure apparent in all the curves; the position of the shock wave is dependent on the combustion-chamber pressure, and hence on the combustion-chamber-inlet Mach number. As the combustion-chamber Mach number is decreased, the shock moves forward to a position of lower intensity, and hence of lower pressure loss, in order to provide the higher combustion-chamber pressures required for continuity. Following the shock, a further rise in static pressure occurs by subsonic diffusion in the

diverging passage. The minor pressure variations apparent in all the curves are due to the presence of the leading edges of the longerons, the fuel manifolds, and the flame holder.

Inasmuch as the condition of maximum pressure recovery, as well as the threshold of significant changes in drag in the flight engine, occurs when the shock is located just at the lip (station 100), the combustion-chamber Mach number that positions the shock at this station is of particular interest. In order to illustrate the nature of the shock in greater detail than is evident in figure 9(a), data were selected from burning runs with configuration 2 in which the shock was positioned near the lip and are presented in figure 9(b). It is apparent from each of these curves that the pressure rise due to the shock occurs over an appreciable length (about 10 in.) and that the pressure-rise process may therefore consist of a single stationary normal shock, an oscillating normal or oblique shock, or some combination of normal and oblique shocks. It is therefore evident that the pressure rise is a complicated process and that an exact definition of the operating point at which the shock moves upstream past the lip is impossible. The actual shock configuration, moreover, is probably not the same as would occur in the flight engine because of the influence of the boundary layer on the inlet-nozzle wall and a nonrepresentative boundary layer on the cone of the test engine. Figure 9(a) shows that the initial pressure rise at the lip occurs for a combustion-chamber Mach number of about 0.15 and that the shock process does not pass completely upstream of the lip until the combustion-chamber Mach number is reduced to a value of about 0.13.

The ratio of the static-pressure drop across the flame holder of configuration 1 to the combustion-chamber-inlet velocity head is shown in figure 10 as a function of combustion-chamber-inlet Mach number. The pressure drop on which these coefficients are based was measured during cold-flow runs by a static-pressure tap located on the inner body about 5 inches upstream of the flame holder and by a static-pressure tap located on the outer shell about 5 inches downstream of the flame holder. The pressure-drop coefficient is independent of the combustion-chamber-inlet Mach number with an average value of about 0.78, as indicated by the faired curve.

The total-pressure-recovery ratio across the subsonic diffuser (between instrument stations 1 and 2) is shown in figure 11. Because of the difficulty in determining the transition point between supersonic and subsonic flow at the lip, points are shown

only for those conditions that are known to be subsonic at the lip. Pressure-recovery ratios ranging from 0.99 to 0.96 were obtained for lip Mach numbers from 0.24 to 0.52. The adiabatic efficiency of the diffuser corresponding to these pressure ratios was about 75 percent.

1282

COMBUSTION RESULTS

The operational limits, combustion performance, and combustion photographs for configurations 1 to 4 are given in figures 12 to 30 and are discussed in the following sections.

Configuration 1

Altitude operational limits. - A plot of the altitude and fuel-air-ratio operating range for configuration 1 is shown in figure 12. Points are shown for operation with the complete flame holder and operation with the flame holder modified by the removal of the two flare cases (fig. 5). The range of fuel-air ratios over which steady burning was possible with the complete flame holder (solid line) decreased rapidly with increasing altitude and varied from about 0.032 to 0.06 at 37,000 feet to a very small range around 0.047 at 48,000 feet. Although the rich blow-out limit was nearly constant for altitudes from 40,000 to 48,000 feet, the lean blow-out limit increased from 0.037 to 0.047 for this increase in altitude. The maximum altitude obtained with this configuration was about 48,000 feet.

The operational limits for the flame holder without flare cases are indicated by the dashed line in figure 12. At an altitude of 40,000 feet, the lean blow-out limit was nearly the same as the limit for the complete flame holder, but the rich blow-out limit was increased from 0.048 to 0.057. Without the flare cases, however, operation was impossible at altitudes greater than about 45,000 feet at any fuel-air ratio.

Combustion temperature and efficiency. - Figure 13 shows the combustion-chamber-outlet temperatures and combustion efficiencies for the operable range of fuel-air ratios at altitudes from 37,000 to 45,000 feet. The combustion temperature increased steadily with fuel-air ratio at all altitudes until blow-out occurred. The combustion efficiencies first increased and then fell off slightly with increasing fuel-air ratios at altitudes of 37,000 and 40,000 feet and decreased as the altitude was increased over

~~CONFIDENTIAL~~

the entire range of fuel-air ratios. The maximum combustion efficiency obtained was about 0.87 at an altitude of 37,000 feet for a fuel-air ratio of about 0.05.

Points are also shown in figure 13 for operation at 40,000 feet without the flare cases. Although a considerably greater scatter is evident in the data without flare cases, the general trend of the points indicates that there is little difference in temperature or combustion efficiency between operation with and without flare cases.

Combustion-chamber pressure, Mach number, and gas-flow data. - The combustion-chamber-outlet total pressure is plotted against the fuel-air ratio in figure 14(a). As the fuel-air ratio increased, the combustion-chamber-outlet pressure increased because of the higher pressure required to pass the mass flow of gas (fixed by the minimum engine-inlet area) through the exit-nozzle throat at the higher gas temperatures. This increase in pressure was, as previously discussed, obtained by a forward shift of the shock wave in the diffuser to a position of lower total-pressure loss. The combustion-chamber pressure ratio P_4/P_2 (fig. 14(b)) was nearly constant at a value of 0.93 for all altitudes over the operable range of fuel-air ratios.

The combustion-chamber-inlet Mach number is plotted in figure 14(c) as a function of fuel-air ratio for a range of altitudes. The Mach number is independent of altitude and decreased with increased fuel-air ratio. Inasmuch as the shock moved upstream past the position of the lip of the engine inlet for combustion-chamber Mach numbers between 0.13 and 0.15, it is evident that all the runs were made with the shock swallowed (downstream of the lip).

In figure 15, the total-gas-flow parameter is plotted against fuel-air ratio. The gas-flow parameter decreased with increased fuel-air ratio over the entire range investigated. Use of this gas-flow parameter correlates data for various altitudes and, for a given flight Mach number, the parameter is a function only of fuel-air ratio and combustion efficiency. In addition to correlating the gas-flow data, this gas-flow parameter is useful in computing values of thrust if the nozzle efficiency is assumed.

Operating characteristics. - In the stable operating range, combustion was smooth and quiet with configuration 1. Blow-out was sudden, occurring with very little warning except an occasional

flicker of the flame or slight roughness. The flame issuing from the exit nozzle was light green in color. The photograph (fig. 30(a)), which was reproduced from the motion pictures taken through the downstream periscope, shows that the flame filled the combustion chamber with the exception of an irregular area in the center of the duct.

2821

Configuration 2

Altitude operational limits. - The altitude and fuel-air-ratio operating range for configuration 2 with the upstream and downstream fuel manifolds located at 20- and 24.6-inch diameters, respectively, is shown in figure 16. Points are shown for both uniform fuel injection in all four quadrants and for injection in two diametrically opposite 90° quadrants only. When only two quadrants were used, injection into quadrants containing the igniter box produced rough, irregular burning. The data presented are therefore for the quadrants that do not contain the igniter box. With uniform injection at altitudes below 45,000 feet, no rich blow-out was obtained for the range of fuel-air ratios investigated (up to 0.067). The lean blow-out limit occurred at a fuel-air ratio of 0.044 at 40,000 feet and 0.047 at 45,000 feet. Operation at altitudes above 48,000 feet was impossible with uniform injection. The use of quadrant injection reduced the fuel-air ratio for lean blow-out to about 0.027 at 40,000 feet and 0.032 at 50,000 feet. At 50,000 feet, an operable range from this lean limit to a fuel-air ratio of 0.045 was possible with quadrant injection.

Altitude operational limits for uniform and quadrant injection with the fuel manifolds located at 21- and 23.6-inch diameters are shown in figure 17. With uniform injection, there was very little change in the operational limits with this change in fuel-manifold position; with quadrant injection, however, the lean blow-out limit at an altitude of 50,000 feet was increased from about 0.031 (fig. 16) to 0.038 (fig. 17).

Combustion temperature and efficiency. - The combustion temperatures and efficiencies for configuration 2 with fuel manifolds located at 20- and 24.6-inch diameters are shown in figure 18. For all quadrant-injection data shown in this figure, the total fuel flow was injected into two opposite quadrants of the fuel manifolds. With uniform injection, combustion temperatures up to about 3800° R were obtained at altitudes of 40,000 and 45,000 feet. The maximum temperature for both these altitudes was reached at a

1282 fuel-air ratio of about 0.065. Combustion efficiencies above 0.90 were obtained for most of the fuel-air ratio range with uniform injection. The combustion efficiencies were considerably lower with quadrant injection (0.6 to 0.7), although higher efficiencies could probably have been obtained in the region of 0.045 over-all fuel-air ratio (0.09 for each quadrant) by reducing the fuel flow to the two rich quadrants and introducing a small amount of fuel to the remaining two quadrants.

The combustion temperature and efficiency obtained with the fuel manifolds located at 21- and 23.6-inch diameters, shown in figure 19, were about 5 to 10 percent lower than for the 20- and 24.6-inch-diameter location. The quadrant-injection data shown in this figure were obtained by starting with injection in two quadrants to give an over-all fuel-air ratio of 0.031 and holding the fuel pressure to these two quadrants constant while increasing the fuel-air ratio in the other two quadrants.

Combustion-chamber pressure, Mach number, and gas-flow data. -

The pressure, Mach number, and gas-flow data for configuration 2 with fuel manifolds located at 20- and 24.6-inch diameters are shown in figures 20 and 21. Trends similar to those of configuration 1 are apparent in all the curves. Because the combustion efficiency was slightly higher for this configuration, the values of the combustion-chamber-outlet total pressure were somewhat higher and the values of combustion-chamber-inlet Mach number and gas-flow parameter were slightly lower than those for configuration 1. Similarly, the values of combustion-chamber-outlet total pressure were lower and the values of combustion-chamber-inlet Mach number and gas-flow parameter were higher for quadrant injection than for uniform injection. The combustion-chamber-inlet Mach numbers approached the values for subsonic lip flow (0.13 to 0.15) at fuel-air ratios around 0.05 for uniform injection. Inasmuch as the operating pressure for each run was set at the bellmouth-nozzle inlet to a value corresponding to the total pressure behind the oblique shock off the central cone of the flight engine, the pressure at the lip position for those operating conditions in which all or part of the shock is upstream of the lip is higher than the pressure required to simulate a flight Mach number of 2.0 at the nominal test altitude. Under these conditions, subcritical operation at an altitude lower than the nominal test altitude indicated in the figures (but at a Mach number of 2.0) is therefore simulated. An alternate flight condition of a higher Mach number than 2.0 at the test altitude would also have been simulated except for an incorrect inlet-air temperature. The magnitude of this error in simulated altitude due to the movement of the shock

ahead of the lip position is, however, estimated to be a maximum of only about 1000 feet for all data presented. In view of the slight effect of this small change in altitude on the combustion efficiency and the operable range of both this configuration and the other configurations to be subsequently presented, these data are considered representative of the performance at the altitudes indicated.

Operating characteristics. - Combustion was smooth for all operating conditions and blow-out occurred suddenly. The color of the flame was similar to that of configuration 1. The photograph (fig. 30(b)) shows that the flame filled the combustion chamber during uniform injection. During quadrant injection, the flame separated into quadrants (fig. 30(c)) with no apparent change in stability or noise level.

Configuration 3

Altitude operational limits. - The altitude and fuel-air-ratio operational range for configuration 3 is shown in figure 22. Rich blow-out was encountered only at an altitude of 50,000 feet for a fuel-air ratio of about 0.065. With uniform injection, the lean blow-out limit varied from about 0.040 at 40,000 feet to 0.048 at 50,000 feet. Operation with quadrant injection reduced the fuel-air ratios for lean blow-out to about 0.028 at 40,000 feet and 0.038 at 50,000 feet. Lean blow-out for annular injection was nearly the same as for quadrant injection at 45,000 feet.

Combustion temperature and efficiency. - The combustion temperatures and efficiencies for configuration 3 are shown in figure 23. The combustion temperatures for all fuel-air ratios were slightly less than those for configuration 2 (fig. 18). For uniform injection, the combustion efficiency was between 0.80 and 0.90 and varied only slightly with fuel-air ratio over the entire range investigated. In general, the combustion efficiency decreased as the altitude was increased from 40,000 to 45,000 feet. Although the scatter in the 50,000-foot-altitude data is large, the average efficiency values are about the same as those for 45,000 feet.

For fuel-air ratios of about 0.034 and below, the quadrant-injection data shown on figure 23 were obtained with only two quadrants operating; for fuel-air ratios higher than 0.034, the data were obtained by starting with two quadrants at a fuel-air ratio of 0.034 and holding the fuel pressure to these two quadrants

constant while increasing the over-all fuel-air ratio with the other two quadrants. The combustion efficiency for quadrant injection decreased with fuel-air ratio up to a fuel-air ratio of about 0.048 and then increased suddenly between fuel-air ratios of 0.048 and 0.051. For fuel-air ratios of 0.051 and higher, the combustion efficiencies obtained with quadrant injection were about the same as those obtained with uniform injection.

For fuel-air ratios of about 0.042 and below, the annular-injection data shown on figure 23 were obtained with only the forward manifold operating; for fuel-air ratios higher than 0.042, the data were obtained by starting with the forward manifold operating at a fuel-air ratio of about 0.042 and holding the fuel pressure to the forward manifold constant while increasing the fuel-air ratio with the rear manifold. The combustion efficiency obtained with this method of fuel injection varied in a regular manner from a value of about 0.40 at a fuel-air ratio of 0.035 to over 0.85 at a fuel-air ratio of 0.067.

Combustion-chamber pressure, Mach number, and gas-flow data. - The pressure, Mach number, and gas-flow data are shown in figures 24 and 25. These data vary in a manner similar to those for previous configurations and have magnitudes similar to those of configuration 2. The engine operates with the shock near the lip for fuel-air ratios greater than about 0.045 (fig. 24(c)).

Operating characteristics. - Operation was smooth and quiet over the entire operating range. The photograph of the combustion with uniform injection (fig. 30(d)) shows that the flame filled the combustion chamber.

Configuration 4

Altitude operational limits. - The rich and lean blow-out limits for configuration 4 (fig. 26) were not greatly affected by altitude in the range from 40,000 feet to 50,000 feet. With uniform injection, the rich limit decreased from about 0.079 to 0.075, and the lean limit increased from 0.04 to 0.042 as altitude increased from 40,000 to 50,000 feet. For runs in which annular injection was used, the lean blow-out limits varied from 0.028 at 40,000 feet to 0.031 at 50,000 feet. The over-all operating range with this configuration was therefore from about 0.031 to 0.075 at 50,000 feet, which closely approaches the design assumptions previously discussed.

Combustion temperature and efficiency. - Combustion temperatures of over 3800° R were obtained with this configuration at an altitude of 40,000 feet and at a fuel-air ratio of about 0.07 (fig. 27(a)). Increasing the altitude to 50,000 feet resulted in about a 5-percent decrease in maximum temperature. The combustion efficiencies for configuration 4 are shown in figure 27(b). With uniform fuel injection, efficiencies above 0.90 were obtained over the greater part of the fuel-air-ratio range at 40,000 feet. At altitudes of 45,000 and 50,000 feet, the efficiency increased from about 0.70 to 0.90 as the fuel-air ratio increased from 0.045 to 0.075. The efficiency with annular injection (all fuel through upstream manifold) varied from 0.53 at a fuel-air ratio of 0.03 to about 0.62 at a fuel-air ratio of 0.036. Within the accuracy of the computations (see appendix B), these combustion efficiencies closely approach the design assumptions at high fuel-air ratios but are considerably lower than the design values at low fuel-air ratios. The effect of these low combustion efficiencies on combustion temperatures in the low fuel-air-ratio range may be offset, however, by operating at fuel-air ratios slightly higher than those of the design specifications.

Combustion-chamber pressure, Mach number, and gas-flow data. - The gas-flow and pressure data are presented in figures 28 and 29. The trends and the magnitude shown are similar to those for configuration 3. Figure 28(c) shows that for uniform injection at all altitudes the combustion-chamber Mach number becomes less than 0.15; hence the shock passes upstream of the lip for fuel-air ratios greater than about 0.05. As previously discussed, however, the error in simulated altitude due to this location of the shock ahead of the lip position is small and both the combustion efficiency and the operational range of this configuration, as shown in figures 26 and 27, are considered representative of the altitudes indicated.

Operating characteristics. - The operating characteristics of configuration 4 were similar to those of the other configurations investigated. Operation was smooth at all altitudes, blow-out occurred suddenly, and the flame was light green in color. With uniform injection, the flame filled the combustion chamber (fig. 30(e)) and with annular injection, the flame was confined to the center of the combustion chamber (fig. 30(f)).

SUMMARY OF RESULTS

An altitude-test-chamber investigation of the combustion performance of a 28-inch ram-jet engine over a range of altitudes for a simulated flight Mach number of approximately 2.0 gave the following results:

1. A flame holder consisting of two annular gutters, each 2 inches wide, and blocking 45 percent of the combustion-chamber area used in conjunction with a double-manifold fuel system having 40 spring-loaded fuel nozzles had a fuel-air-ratio range of stable operation from 0.031 to 0.075 at an altitude of 50,000 feet. For lean operation (0.031 to 0.040), only one manifold was used to provide annular injection, but for rich operation (0.042 to 0.075), both manifolds were used to provide uniform injection.

2. Combustion efficiencies with this configuration varied from 0.53 to 0.62 with annular injection for fuel-air ratios from 0.030 to 0.036 to over 0.90 with uniform injection for fuel-air ratios of about 0.065.

3. Within the accuracy of the computations, the combustion efficiency at high fuel-air ratios with this configuration very closely approached the values assumed in the engine design. At low fuel-air ratios, however, the combustion efficiency was somewhat lower than the design assumptions, but the required temperature may be obtained by operating at higher fuel-air ratios.

4. Three additional configurations employing different fuel systems and two flame holders with blocked areas of 42 and 55 percent had combustion efficiencies nearly equal to or slightly higher than those previously presented for some operating conditions; however, the operating fuel-air-ratio range was inferior at altitudes above 40,000 feet.

5. Combustion was smooth and quiet for all configurations within the operating range. Blow-out occurred suddenly and without appreciable decrease in stability as blow-out fuel-air ratios were approached. The flame filled the combustion chamber for most configurations.

Lewis Flight Propulsion Laboratory,
National Advisory Committee for Aeronautics,
Cleveland, Ohio.

APPENDIX A

SYMBOLS

The following symbols are used throughout the report:

A	area, sq ft
g	acceleration due to gravity, ft/sec ²
M	Mach number
P	total pressure, lb/sq ft absolute
p	static pressure, lb/sq ft absolute
q	dynamic pressure, lb/sq ft
R	gas constant, ft-lb/(lb)(°R)
T	total temperature, °R
t	static temperature, °R
V	velocity, ft/sec
W _t	total weight flow of air plus fuel, lb/sec
γ _{av}	average ratio of specific heats between total and static temperature at exit-nozzle throat
γ _s	ratio of specific heats at static temperature at exit-nozzle throat
η _b	combustion efficiency

Subscripts:

0	conditions at engine inlet (station 69)
1	conditions at plane of simulated cowl lip (station 100)
2	conditions at combustion-chamber inlet (station 297)

- 2' conditions at station 2 adjusted to combustion-chamber area
- 4 conditions at combustion-chamber outlet (station 349)
- 5 conditions at exhaust-nozzle throat (station 366)

1282

APPENDIX B

CALCULATIONS

Calculation of Combustion-Chamber-Outlet Temperature

The combustion-chamber-outlet temperature was calculated from the following equation, which was derived from the conventional compressible-flow equations for a choked nozzle when T_4 is assumed equal to T_5 :

$$T_4 = \frac{P_5^2 A_5^2 g \gamma_s (\gamma_{av} + 1)}{W_t^2 2R} \quad (B1)$$

A value of T_4 is first estimated from the measured fuel-air ratio and the values of R , γ_s , and γ_{av} are evaluated for this temperature. A first approximation for T_4 is then calculated from equation (B1) and, if necessary, the values of γ are recalculated and a second calculation of T_4 is made. In equation (B1) the effective flow area A_5 has been assumed equal to the geometrical area. Although the temperatures computed from equation (1) may be somewhat high because of failure to include an area coefficient, it is believed that any error would be substantially independent of configuration and that temperature values obtained would be adequate for relative comparison.

In addition to equation (1), the following equation can be used for calculation of T_4 :

$$T_4 = \frac{P_5^2 g A_5^2}{W_t^2 R} \left\{ \frac{2\gamma_{av}}{\gamma_{av} - 1} \left(\frac{P_4}{P_5} \right)^{\frac{\gamma_{av}-1}{\gamma_{av}}} \left[\left(\frac{P_4}{P_5} \right)^{\frac{\gamma_{av}-1}{\gamma_{av}}} - 1 \right] \right\} \quad (B2)$$

In the derivation of the equation it was assumed that no loss in total pressure occurred between P_4 and P_5 . Values of T_4 computed from equation (B2) varied as much as 15 percent from those calculated from equation (B1), and their use in calculations of combustion efficiency resulted in values greater than 100 percent on frequent occasions. These discrepancies are believed to be caused principally by the use of the nozzle-inlet total pressure P_4 instead of the proper value at the nozzle throat, inasmuch

as in equation (B2) losses in total pressure between the nozzle inlet and nozzle throat due to wall friction and burning would result in an erroneously high combustion temperature. As a result, the combustion temperatures reported herein were calculated from equation (B1).

Calculation of Combustion Efficiency

The combustion efficiency was calculated from the following equation:

$$\eta_b = \frac{(T_4 - T_1)}{\Delta T_{\text{ideal}}} \quad (\text{B3})$$

where ΔT_{ideal} is the ideal temperature rise corresponding to the fuel-air ratio. This temperature rise was obtained from the theoretical curves in reference 3.

This definition of combustion efficiency was chosen in preference to the definition based on enthalpy ratios because of its relative simplicity and because check calculations of several test points up to stoichiometric mixtures showed little significant difference between the two methods.

REFERENCES

1. Barson, Zelmar, and Wilsted, H. D.: Altitude-Chamber Performance of British Rolls-Royce Nene II Engine. I - Standard 18.75-Inch-Diameter Jet Nozzle. NACA RM E9I23, 1949.
2. Essig, Robert H., Bohanon, H. R., and Gabriel, David S.: Jet Diffuser for Simulating Ram-Pressure and Altitude Conditions on a Turbojet-Engine Static Test Stand. NACA TN 1687, 1948.
3. Mulready, Richard C.: The Ideal Temperature Rise Due to the Constant Pressure Combustion of Hydrocarbon Fuels. Meteor Rep. UAC-9, Res. Dept., United Aircraft Corp., July 1947. (Proj. Meteor, Bur. Ord. Contract NOrd 9845 in cooperation with M.I.T.)

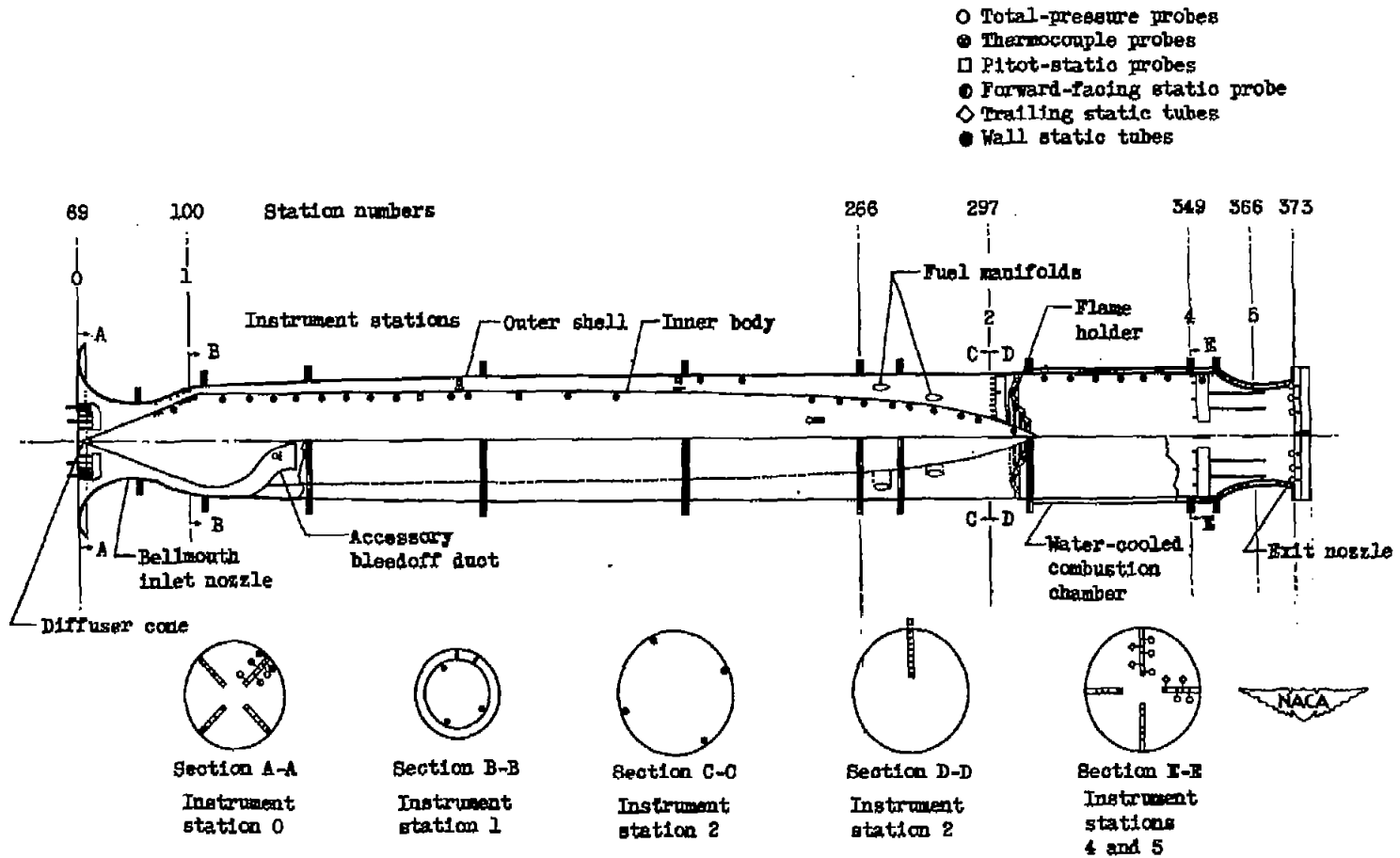


Figure 1. - Schematic diagram of 28-inch ram-jet engine showing instrumentation and station locations.

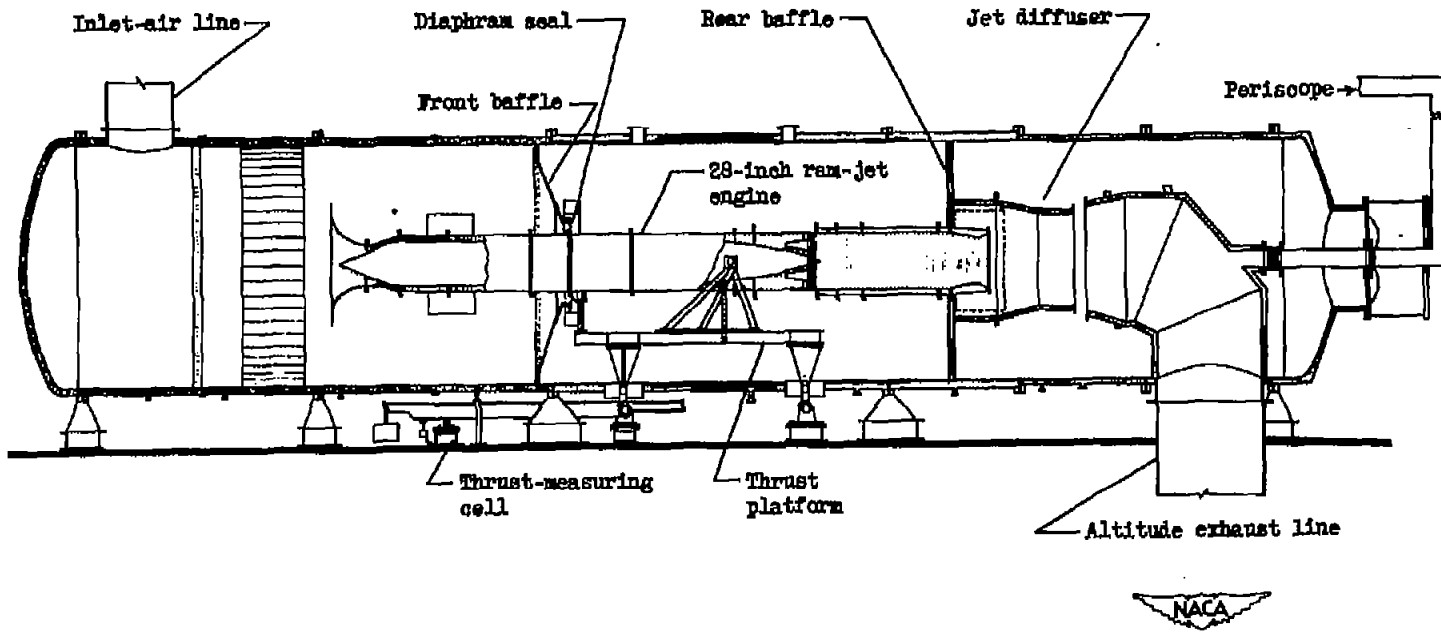


Figure 2. - Schematic diagram of 28-inch ram-jet engine installed in 10-foot altitude test chamber.



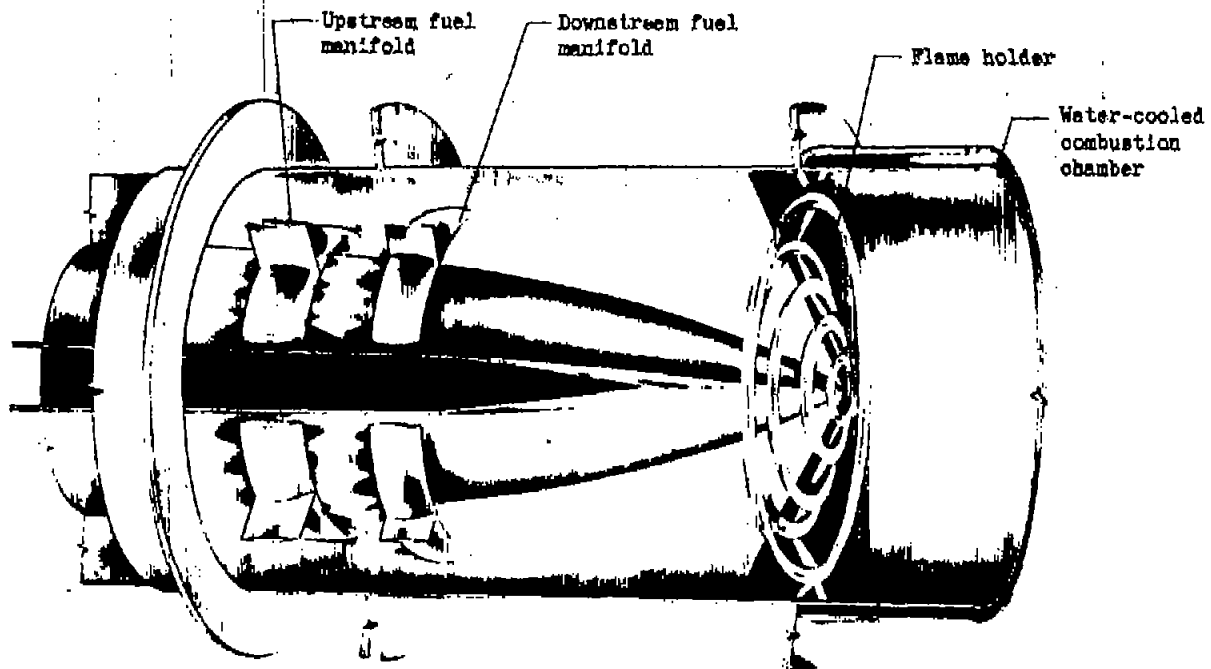
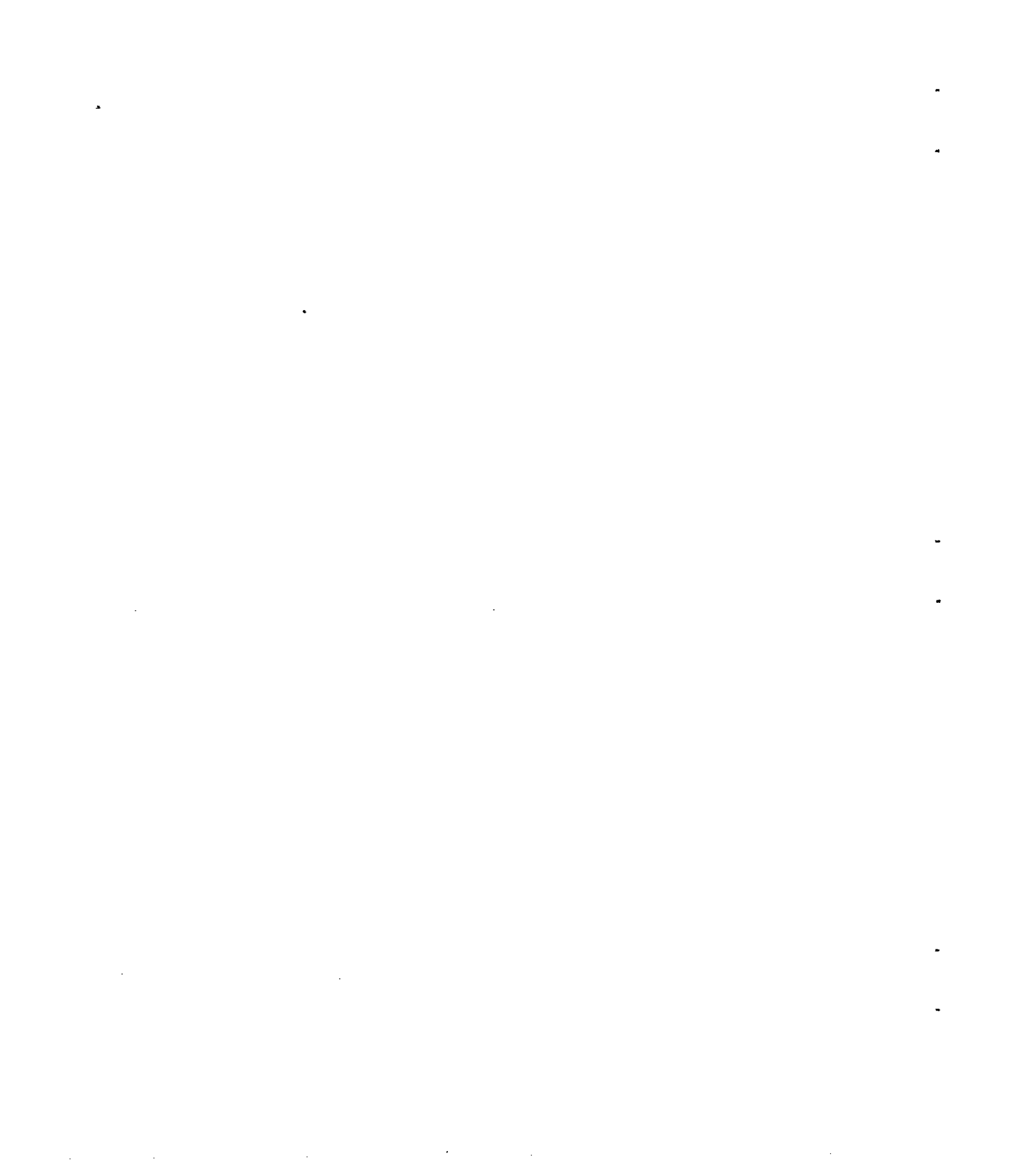


Figure 3. - Schematic diagram of fuel-injection system, flame holder, and combustion chamber for 28-inch ram-jet engine.





1282

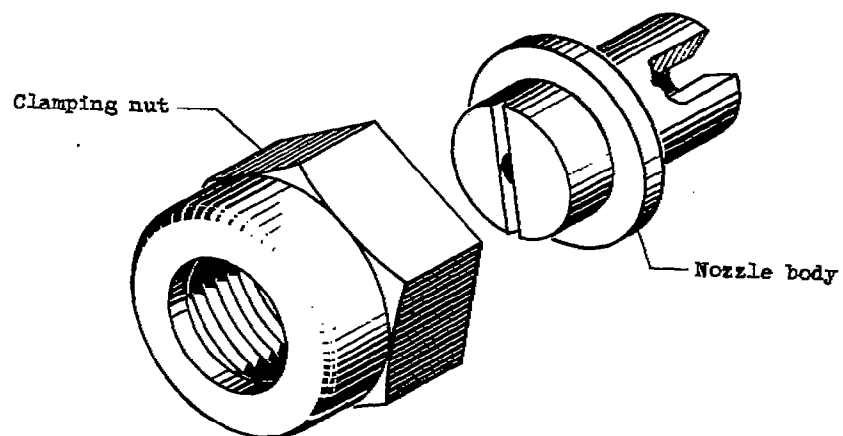


Figure 4. - Flat-spray nozzle.

431-1815

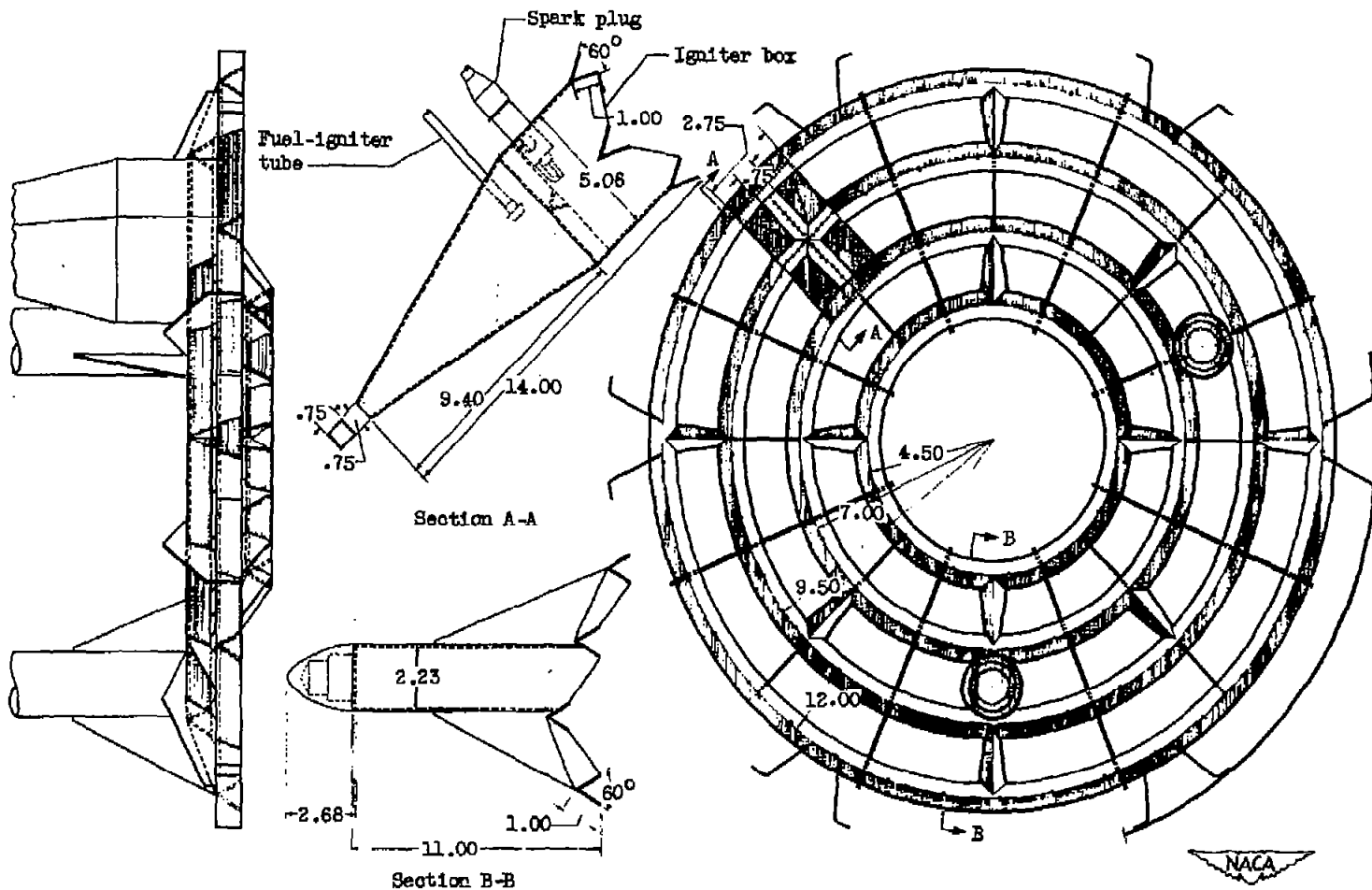


Figure 5. - Schematic diagram of flame holder for configurations 1 and 2. Gutter width, 1 inch; blocked area, 42 percent. (All dimensions in inches unless otherwise indicated.)

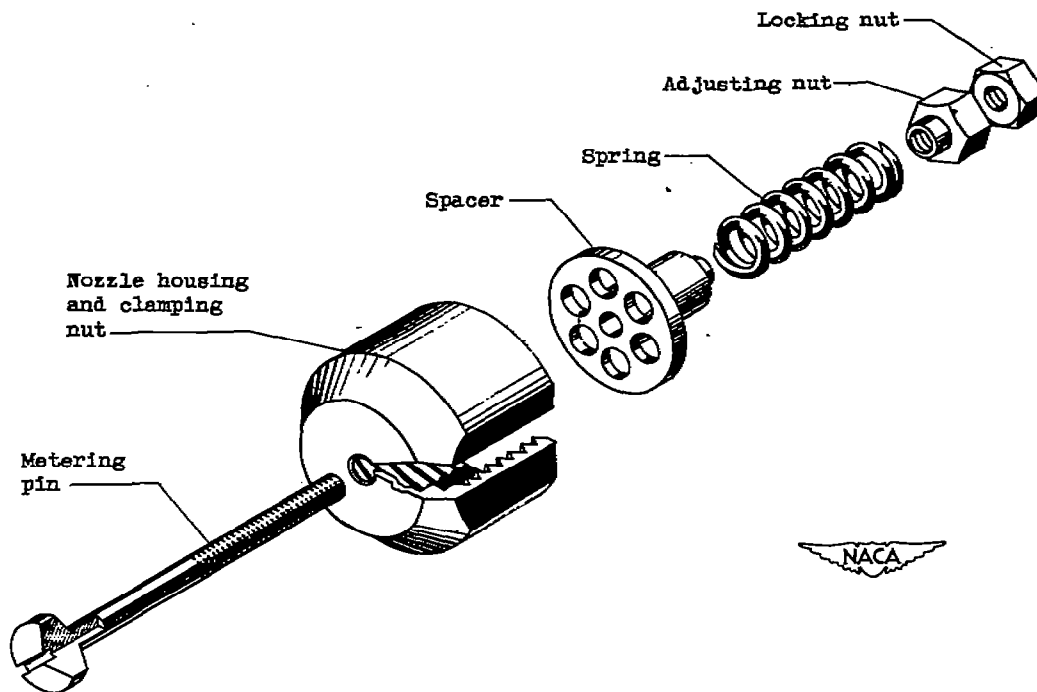


Figure 6. - Details of spring-loaded nozzle.

1282

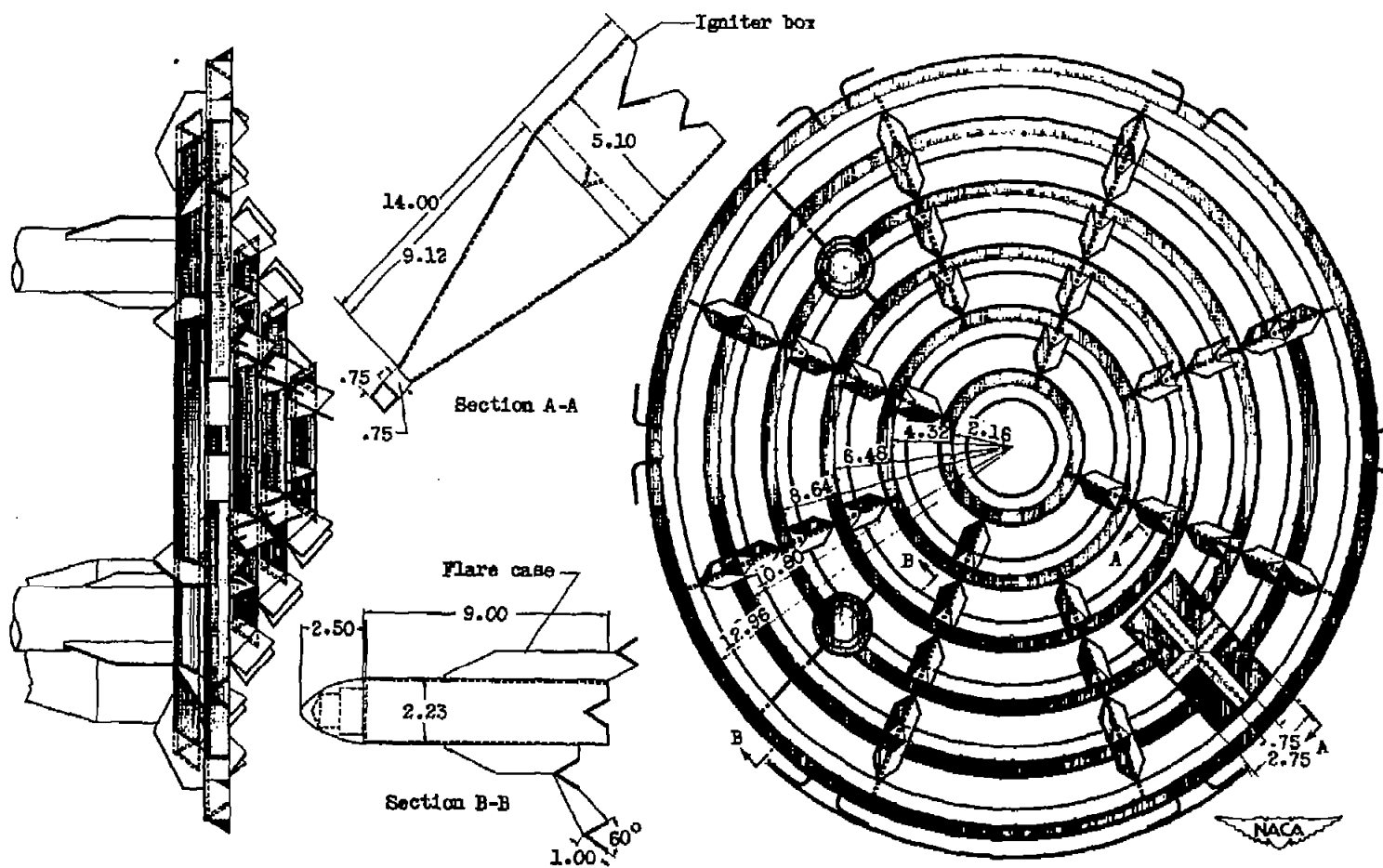


Figure 7. - Schematic diagram of flame holder for configuration 5. Gutter width, 1 inch; blocked area, 55 percent. (All dimensions in inches unless otherwise indicated.)

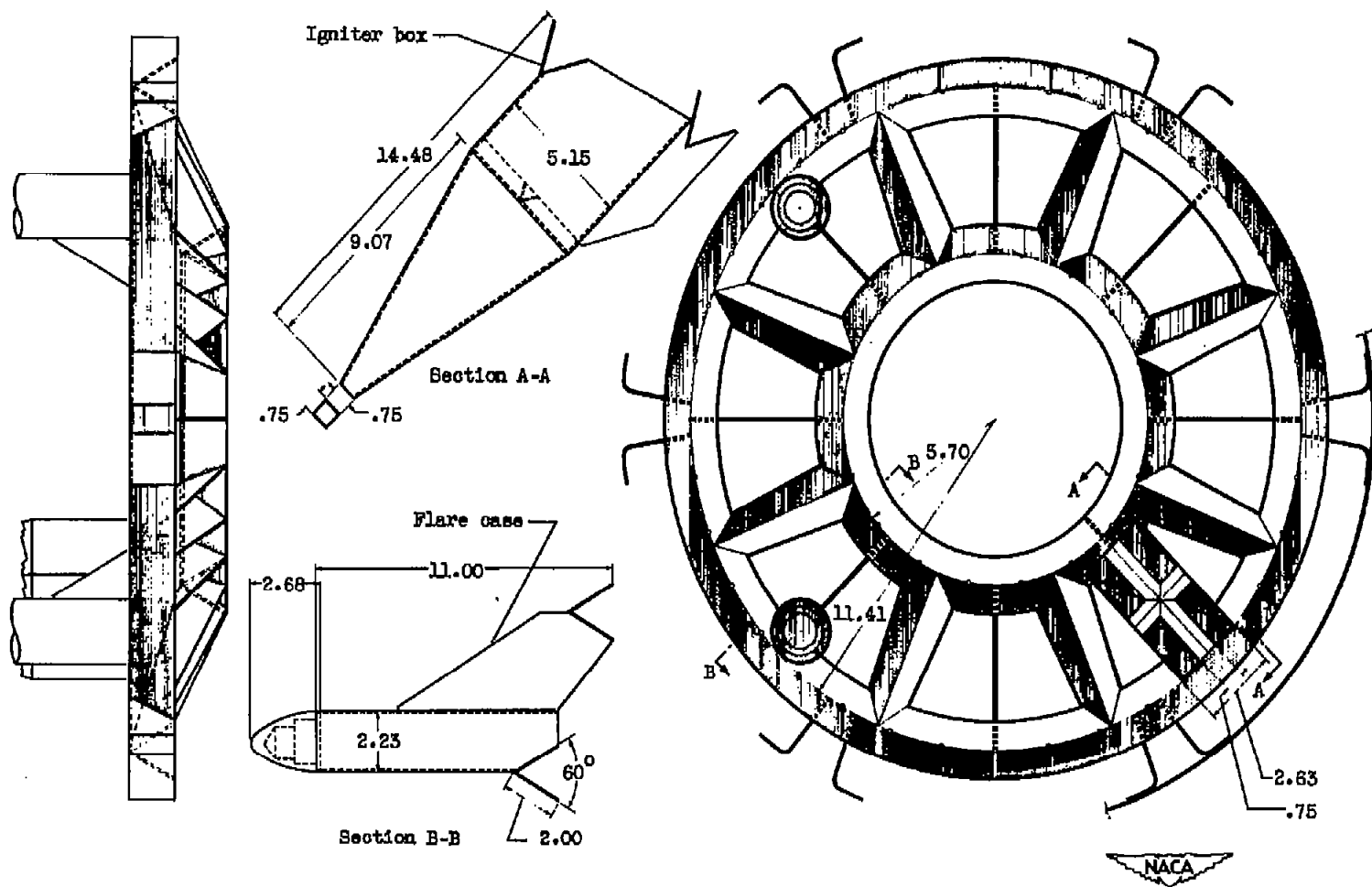
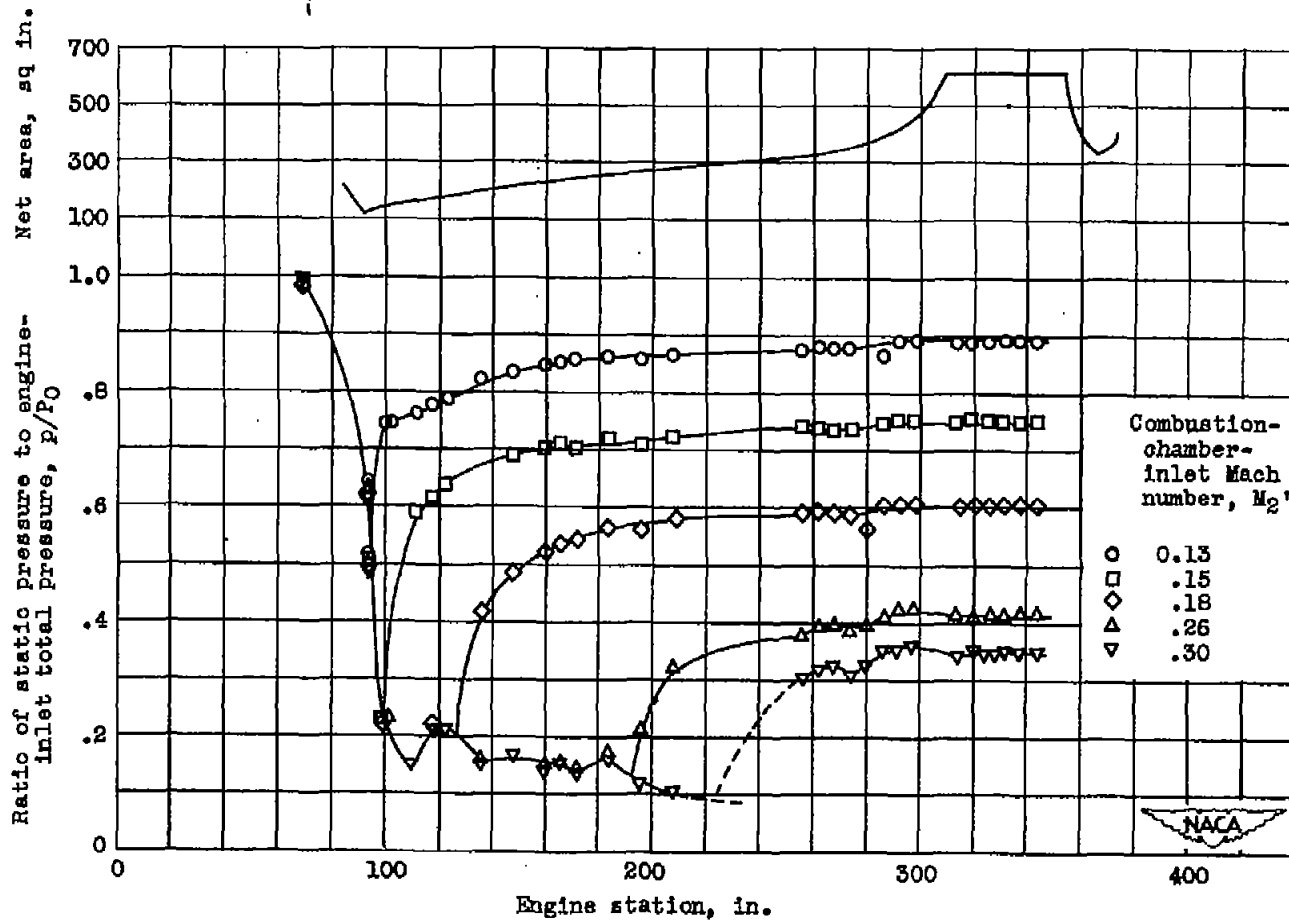


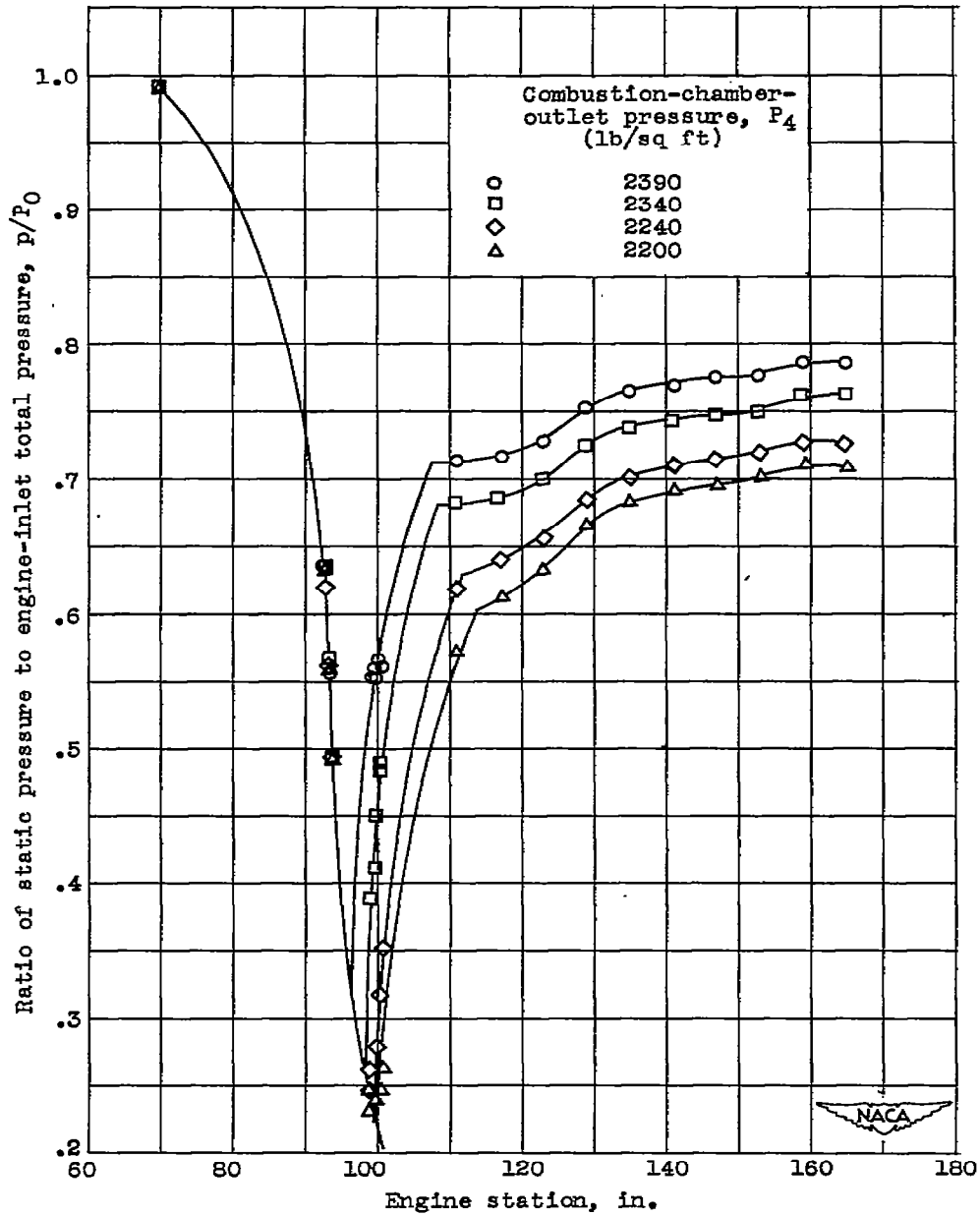
Figure 8. - Schematic diagram of flame holder for configuration 4. Gutter width, 2 inches; blocked area, 45 percent. (All dimensions in inches unless otherwise indicated.)



(a) Configuration 1, without burning.

Figure 9. - Static-pressure distribution along engine.

1282



(b) Configuration 2, with burning.

Figure 9. - Concluded. . Static-pressure distribution along engine.

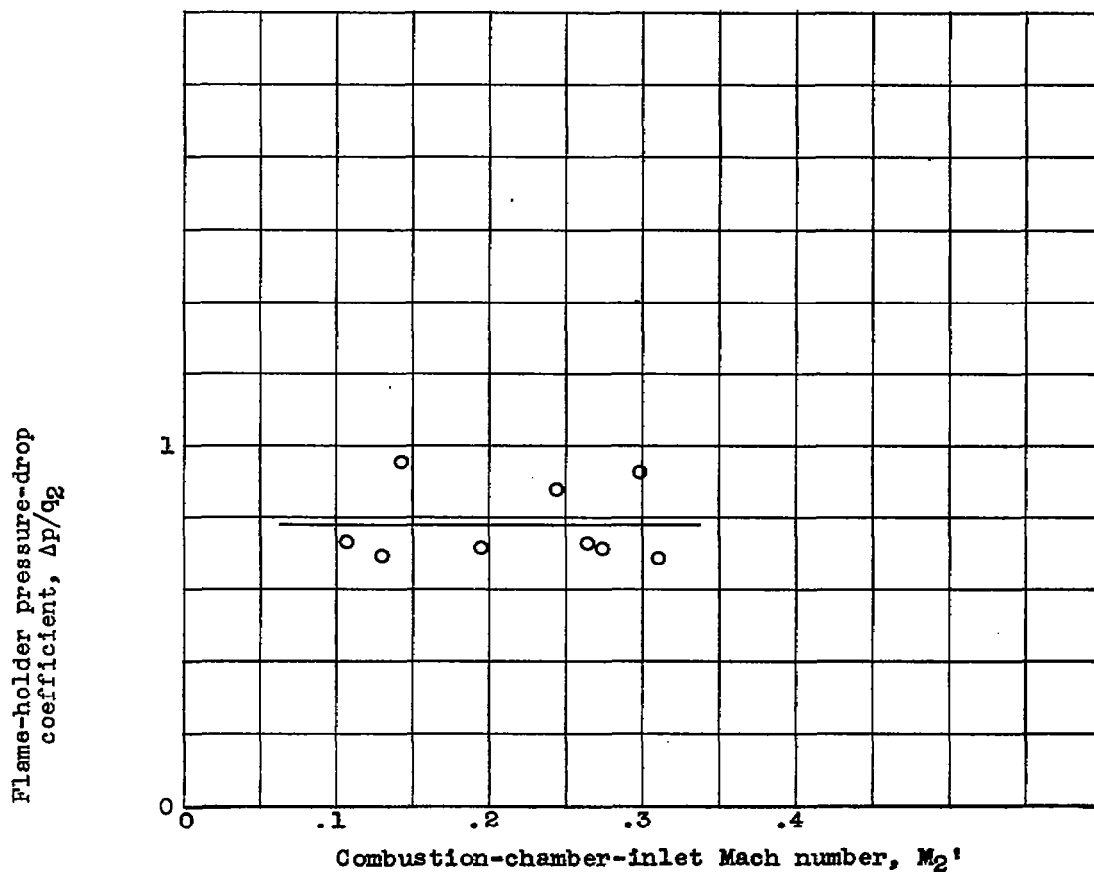


Figure 10. - Flame-holder pressure-drop coefficients without burning, configuration 1.

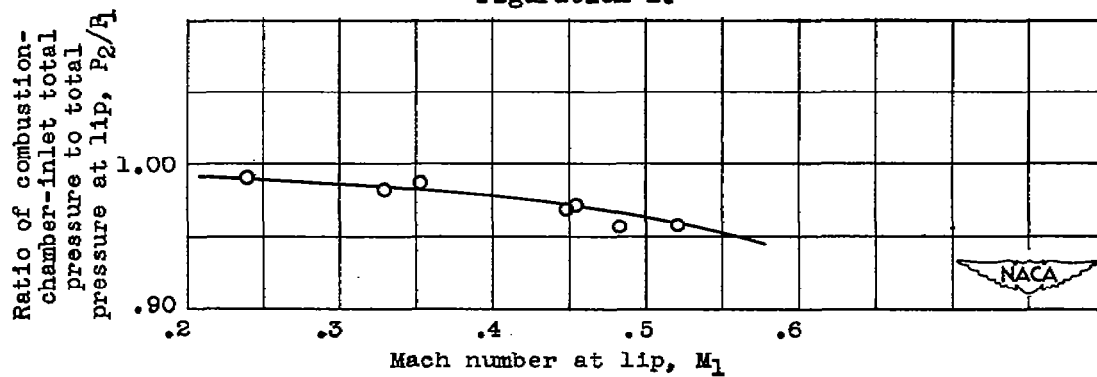


Figure 11. - Subsonic-diffuser pressure recovery for subsonic operating range, no burning.

1282

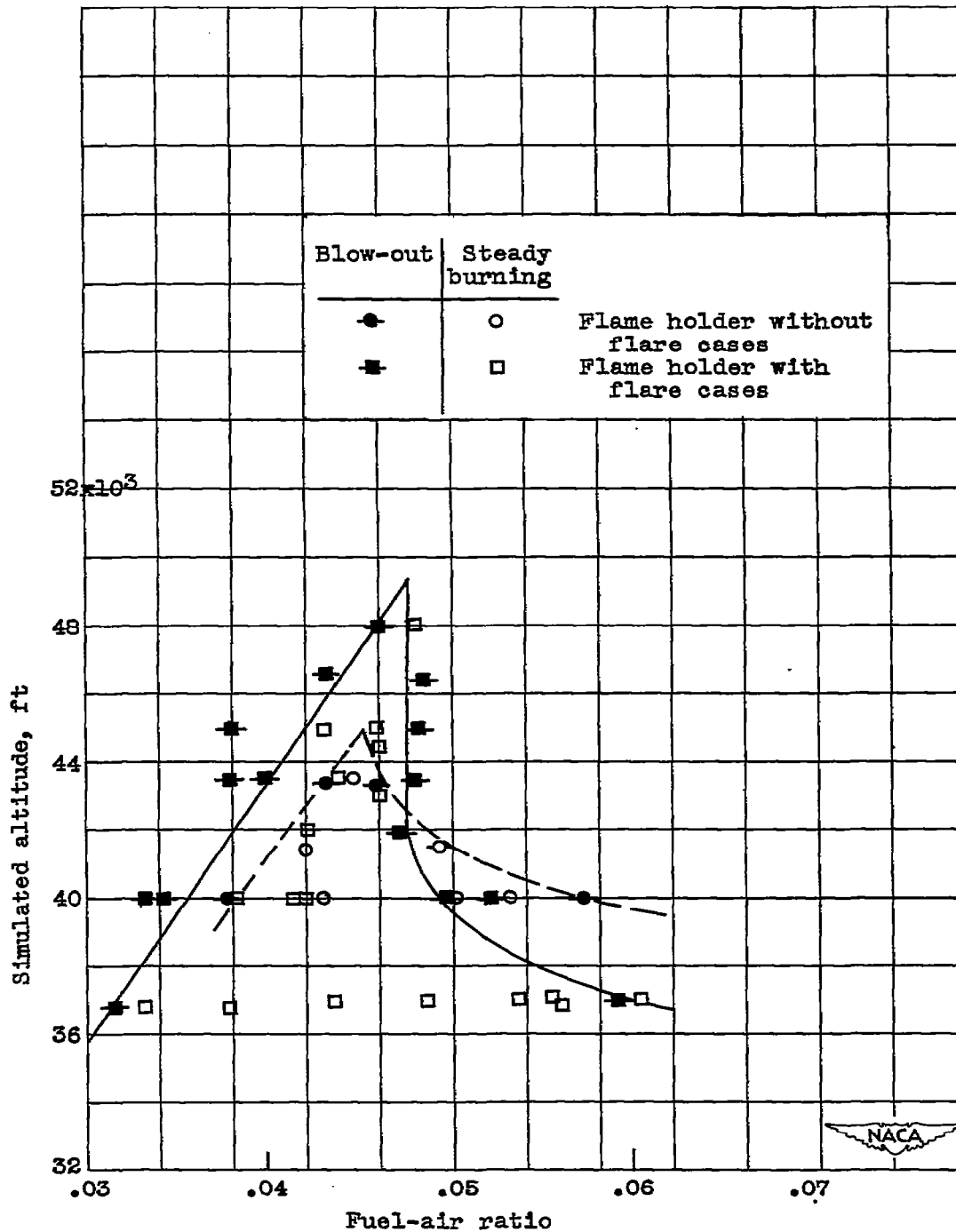
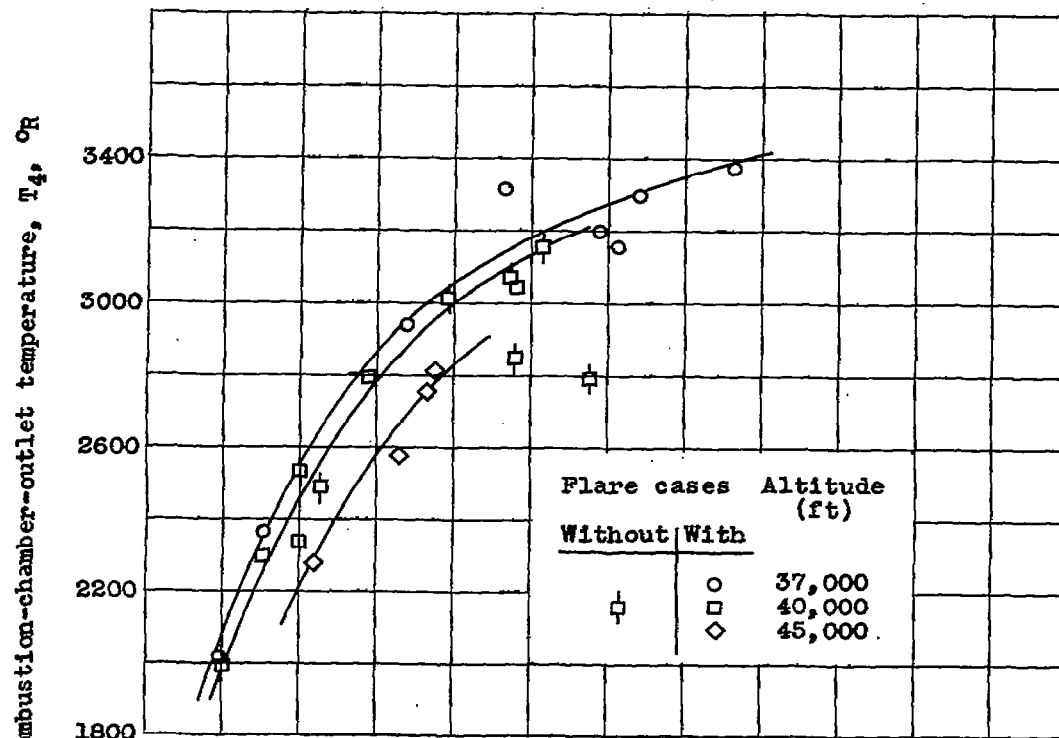
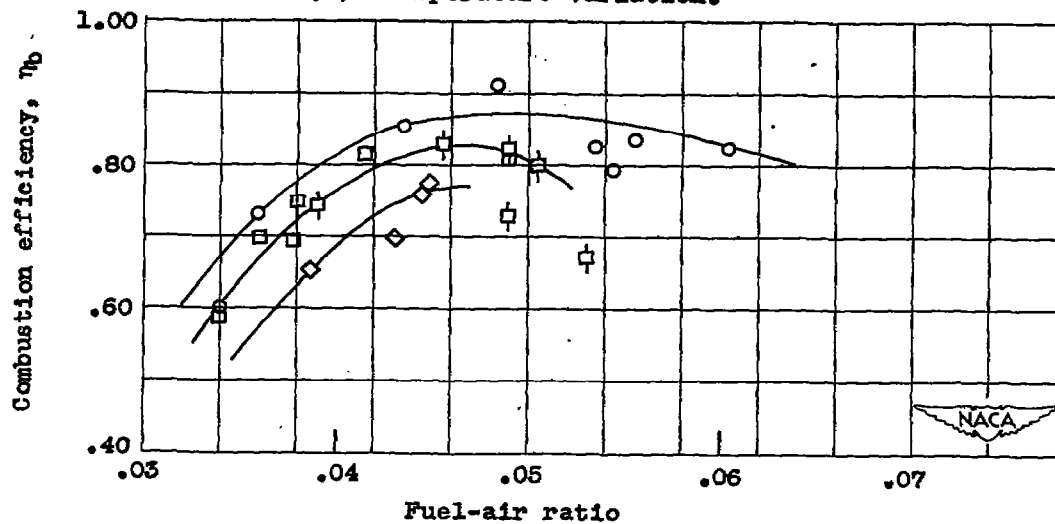


Figure 12. - Operational limits for configuration 1. Single-manifold fuel system using fixed-area fuel nozzles and flame holder with 1-inch wide gutters and 42-percent blocked area.

CONFIDENTIAL



(a) Temperature variation.



(b) Combustion-efficiency variation.

Figure 13. - Variation of combustion-chamber-outlet temperature and combustion efficiency with fuel-air ratio for configuration 1. Single-manifold fuel system using fixed-area fuel nozzles and flame holder with 1-inch wide gutters and 42-percent blocked area.

2827

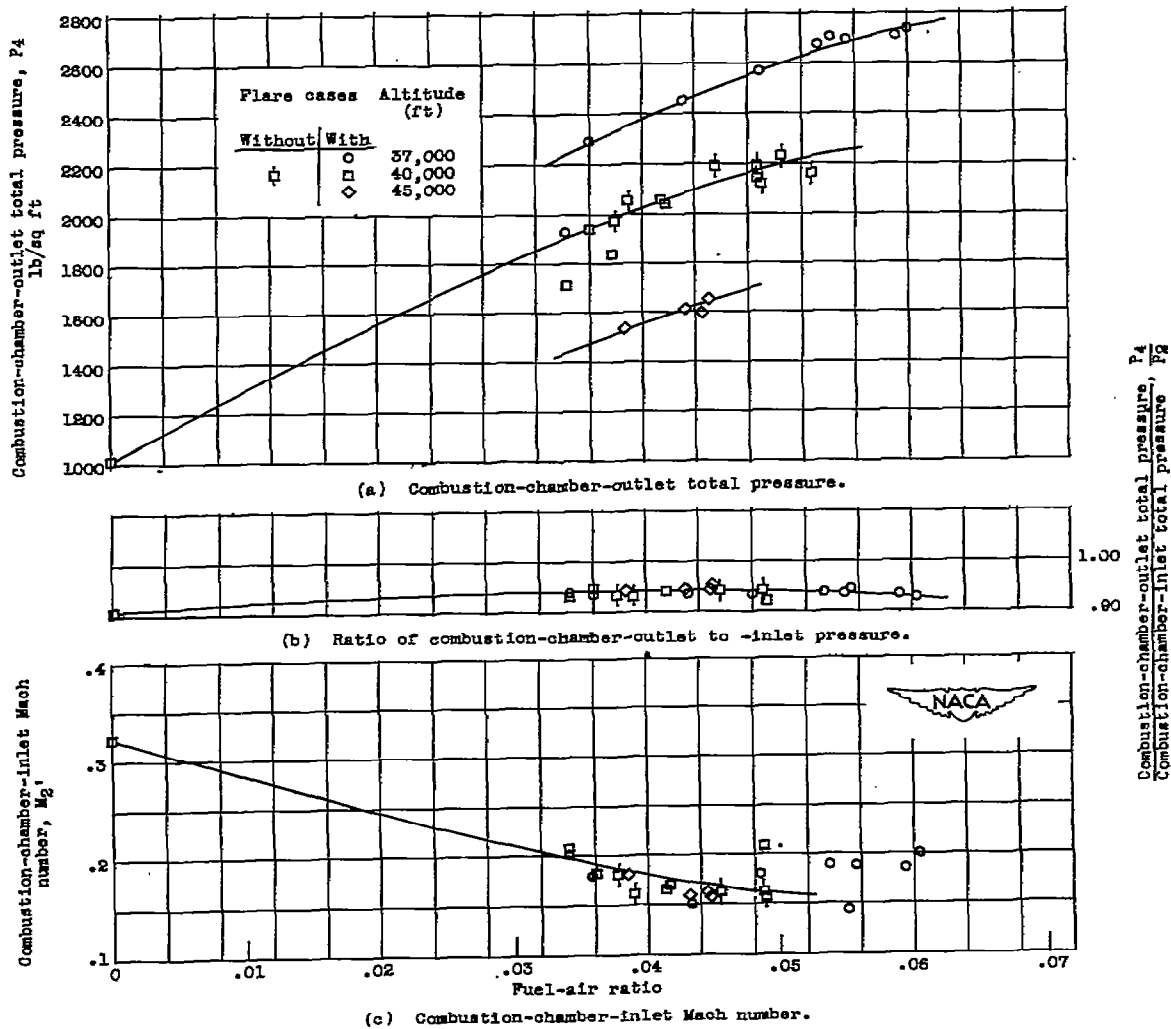


Figure 14. - Variation of engine pressures and Mach numbers with fuel-air ratio for configuration 1. Single-manifold fuel system using fixed-area fuel nozzles and flame holder with 1-inch wide gutters and 42-percent blocked area.

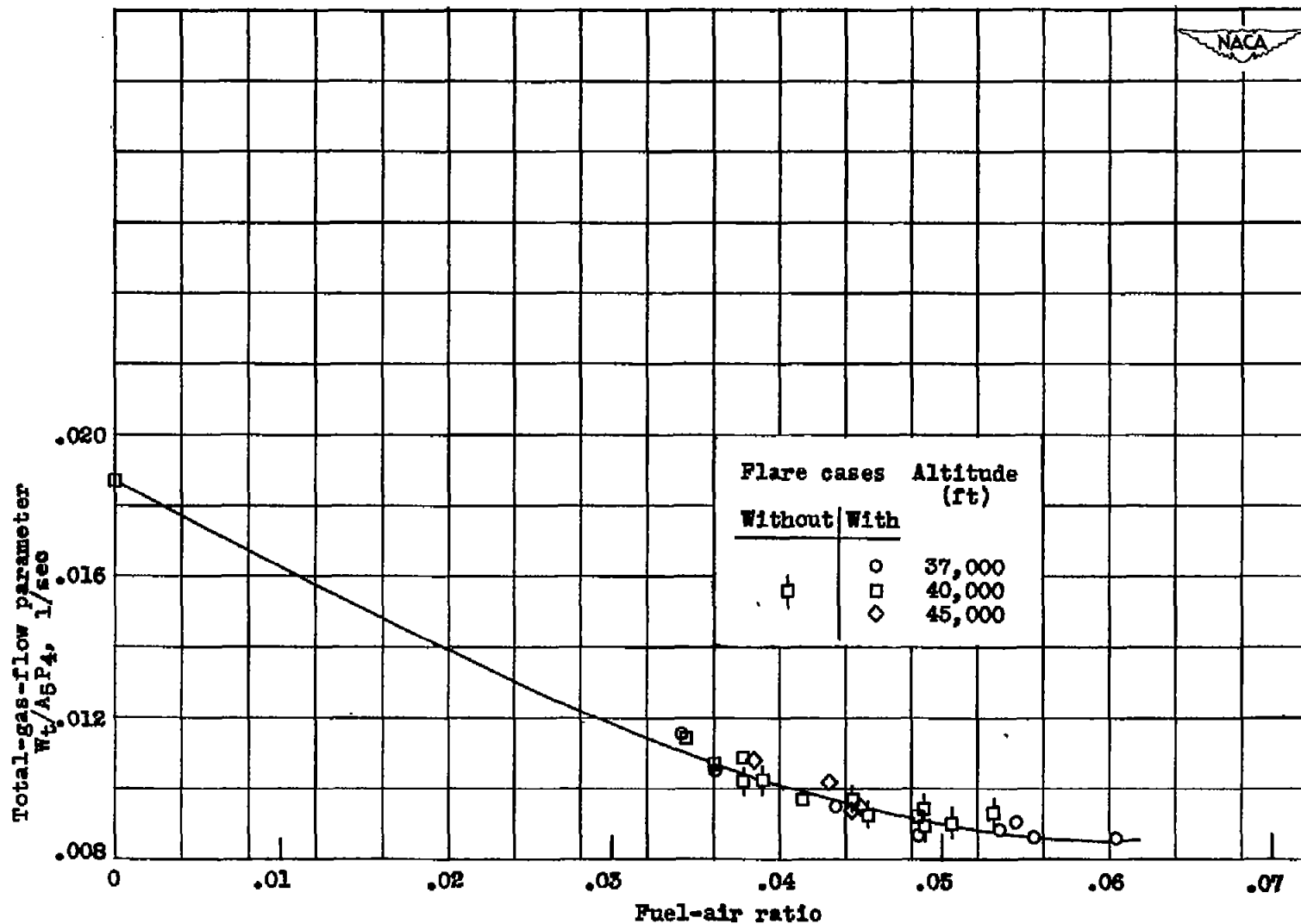


Figure 15. - Gas-flow correlation for configuration 1. Single-manifold fuel system using fixed-area fuel nozzles and flame holder with 1-inch wide gutters and 42-percent blocked area.

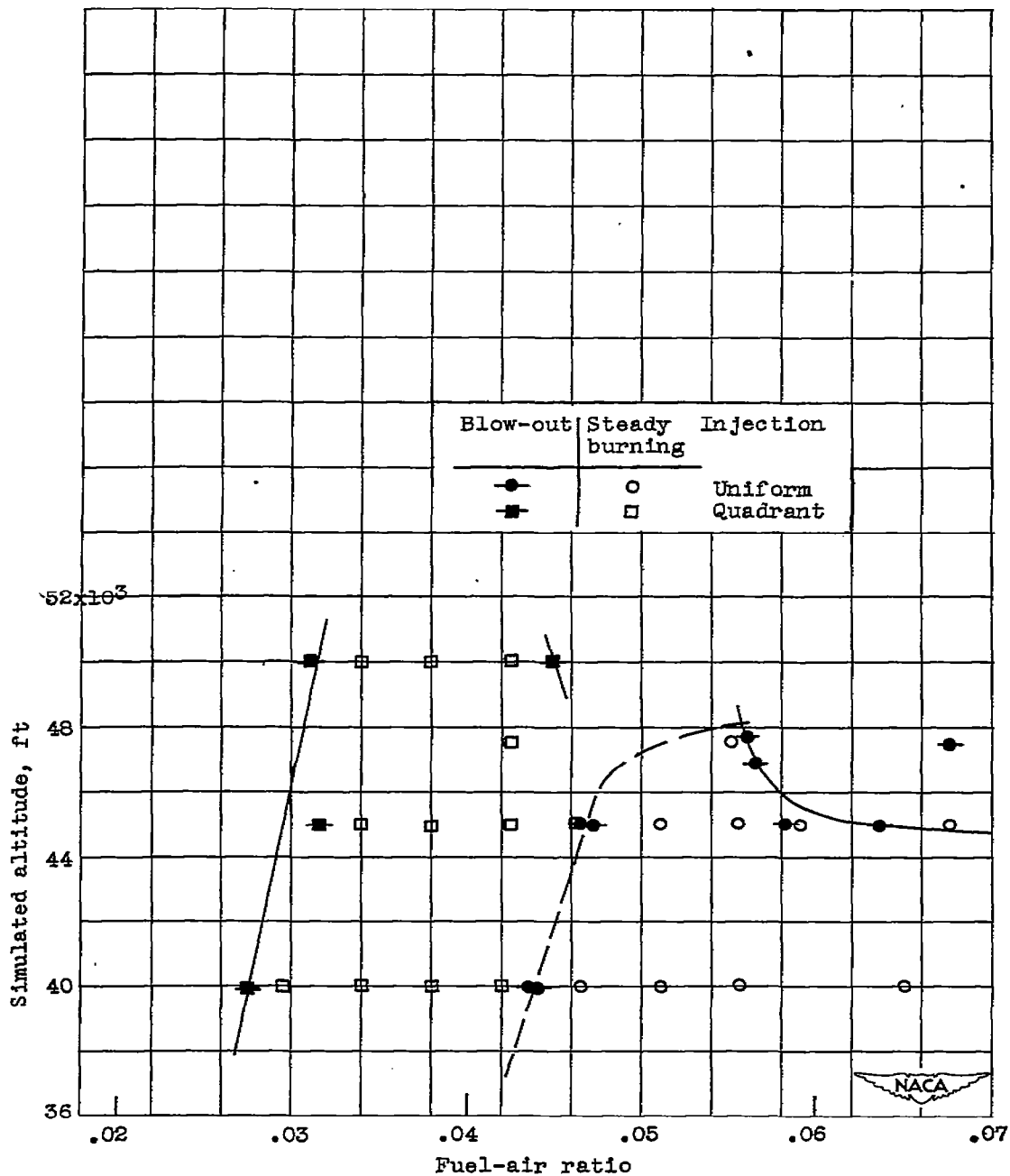


Figure 16. - Operational limits for configuration 2. Double-manifold fuel system with manifolds located at 20- and 24.6-inch diameters using variable-area, spring-loaded fuel nozzles and flame holder with 1-inch wide gutters and 42-percent blocked area.

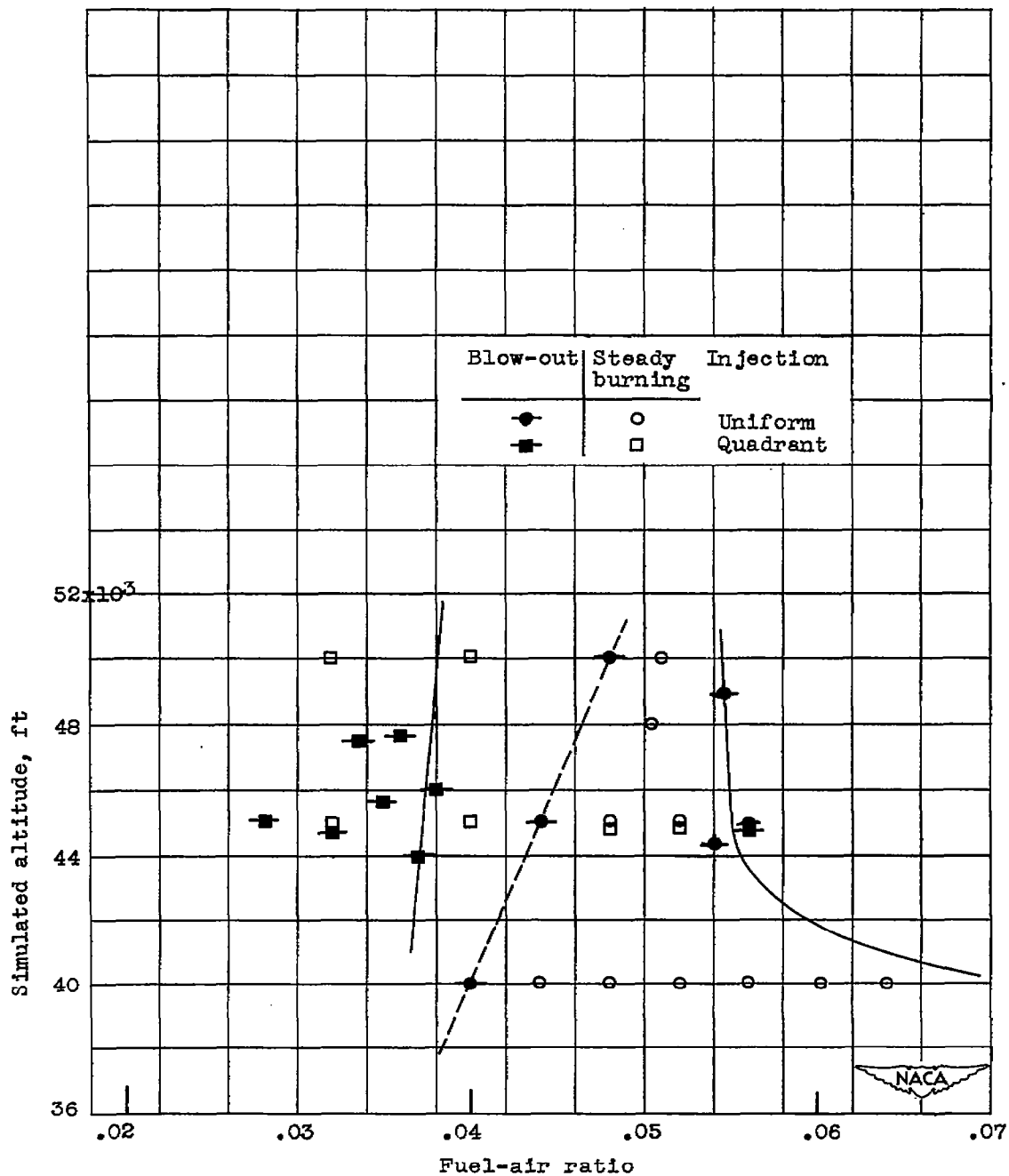
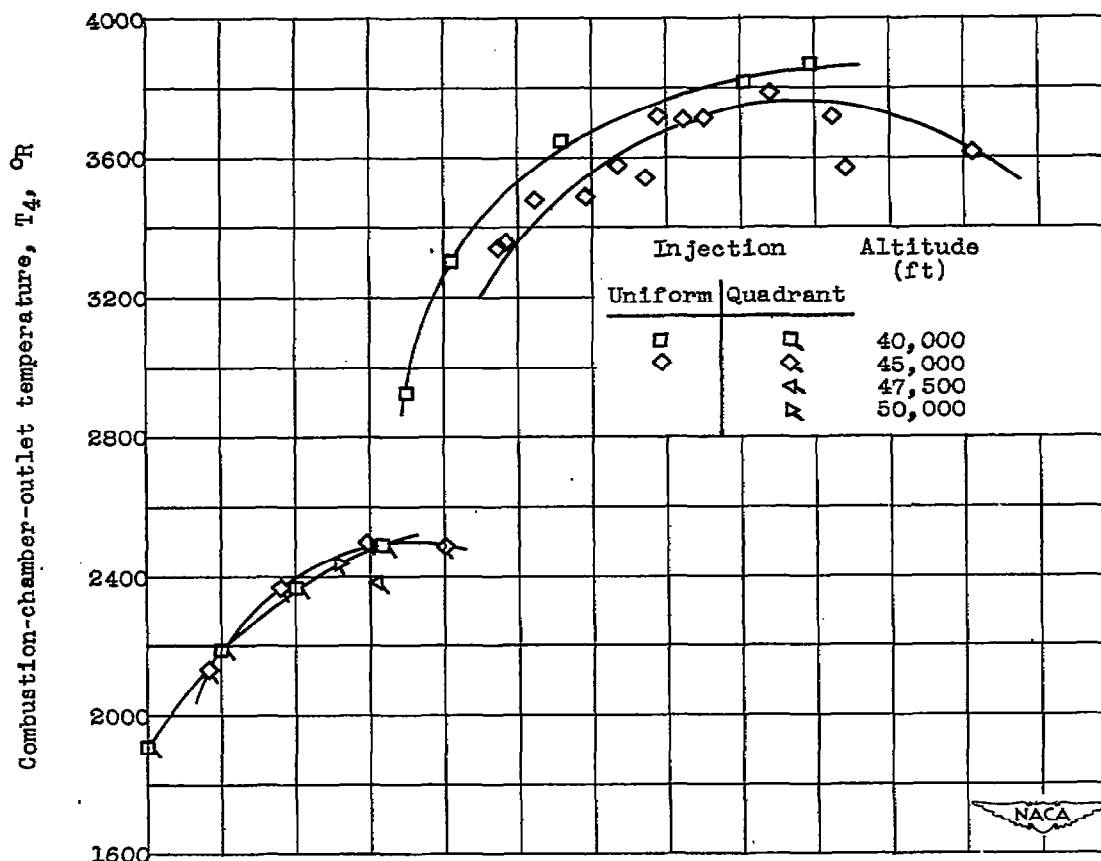
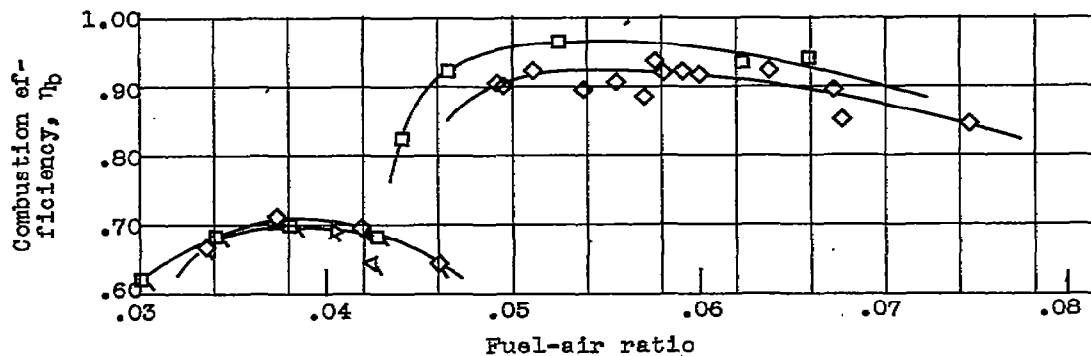


Figure 17. - Operational limits for configuration 2. Double-manifold fuel system with manifolds located at 21- and 23.6-inch diameters using variable-area, spring-loaded fuel nozzles and flame holder with 1-inch wide gutters and 42-percent blocked area.

1282

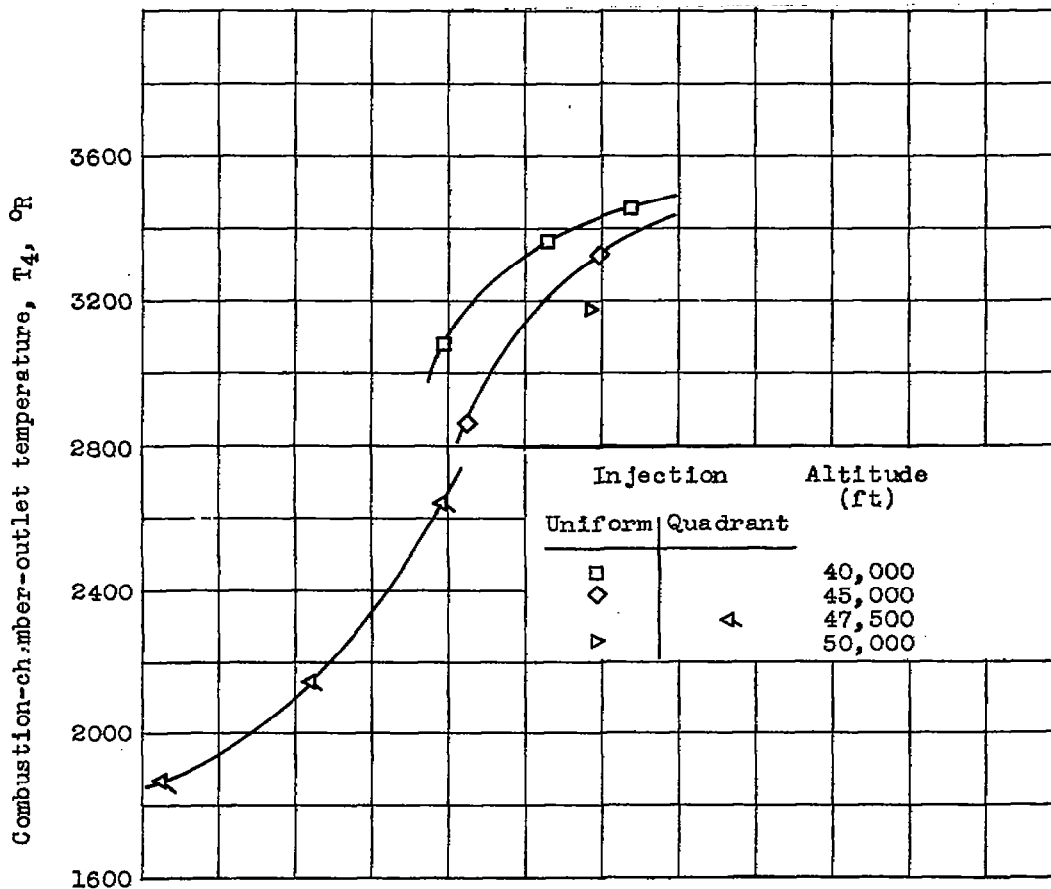


(a) Temperature variation.

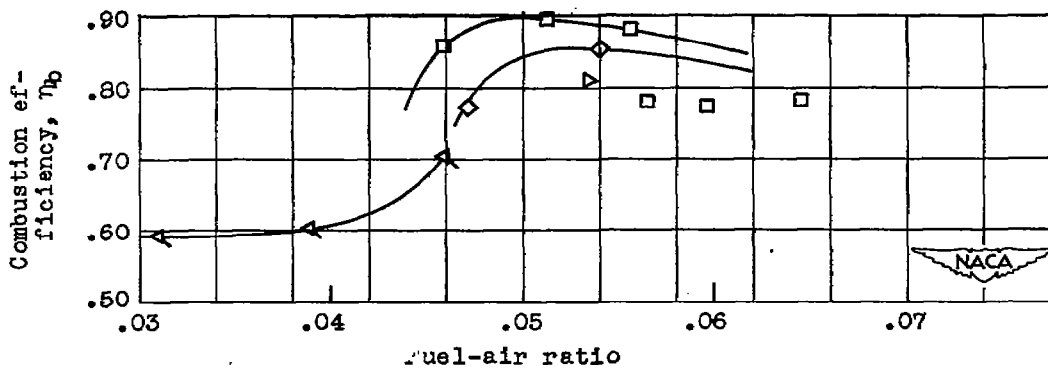


(b) Combustion-efficiency variation.

Figure 18. - Variation of combustion-chamber-outlet temperature and combustion efficiency with fuel-air ratio for configuration 2. Double-manifold fuel system with manifolds located at 20- and 24.6-inch diameters using variable-area, spring-loaded fuel nozzles and flame holder with 1-inch wide gutters and 42-percent blocked area.



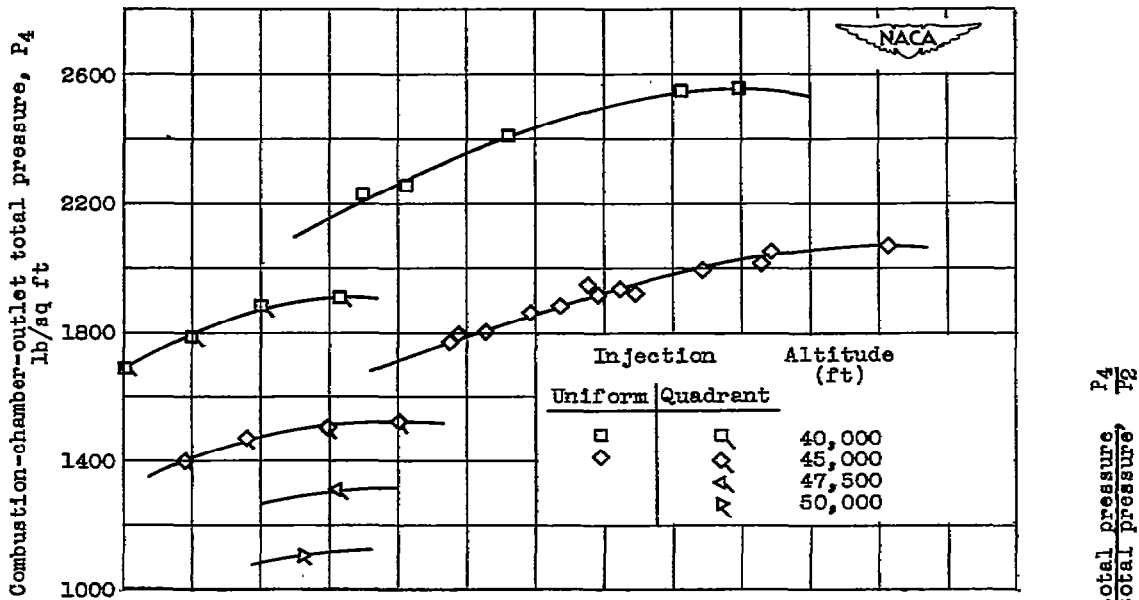
(a) Temperature variation.



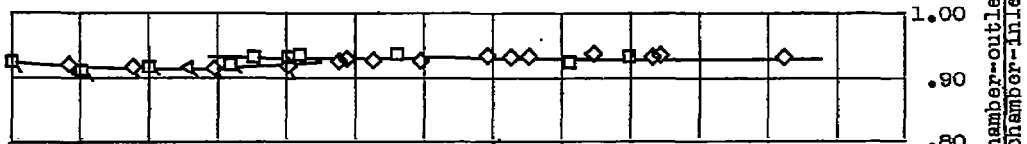
(b) Combustion-efficiency variation.

Figure 19. - Variation of combustion-chamber-outlet temperature and combustion efficiency with fuel-air ratio for configuration 2. Double-manifold fuel system with manifolds located at 21- and 23.6-inch diameters using variable-area, spring-loaded fuel nozzles and flame holder with 1-inch wide gutters and 42-percent blocked area.

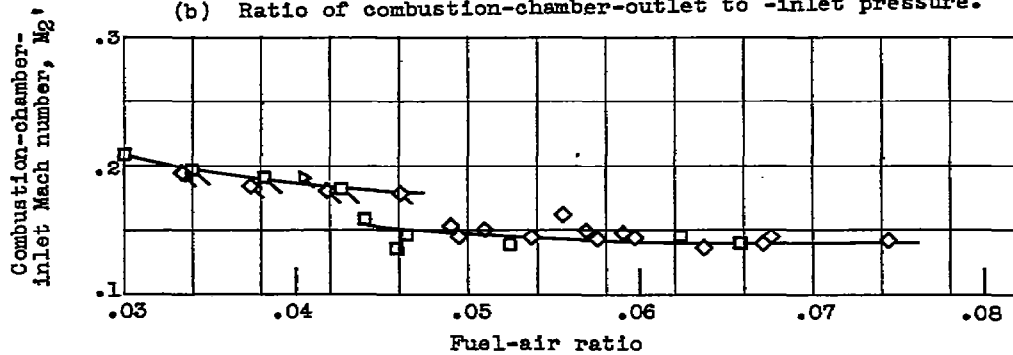
1282



(a) Combustion-chamber-outlet pressure variation.



(b) Ratio of combustion-chamber-outlet to -inlet pressure.



(c) Combustion-chamber-inlet Mach number.

Figure 20. - Variation of engine pressures and Mach numbers with fuel-air ratio for configuration 2. Double-manifold fuel system with manifolds located at 20- and 24.6-inch diameters using variable-area, spring-loaded fuel nozzles and flame holder with 1-inch wide gutters and 42-percent blocked area.

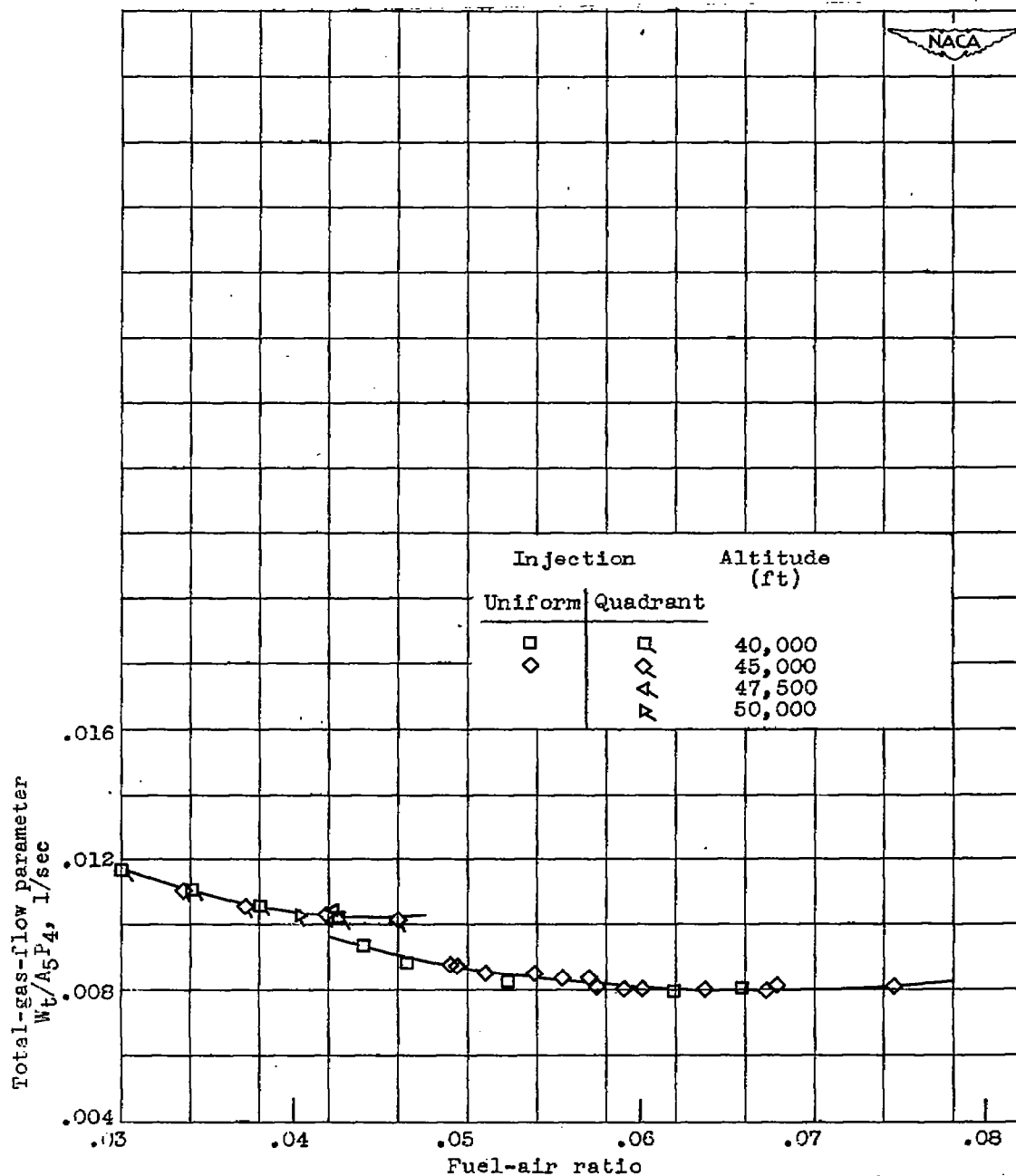


Figure 21. - Gas-flow correlation for configuration 2. Double-manifold fuel system with manifolds located at 20- and 24.6-inch diameters using variable-area, spring-loaded fuel nozzles and flame holder with 1-inch wide gutters and 42-percent blocked area.

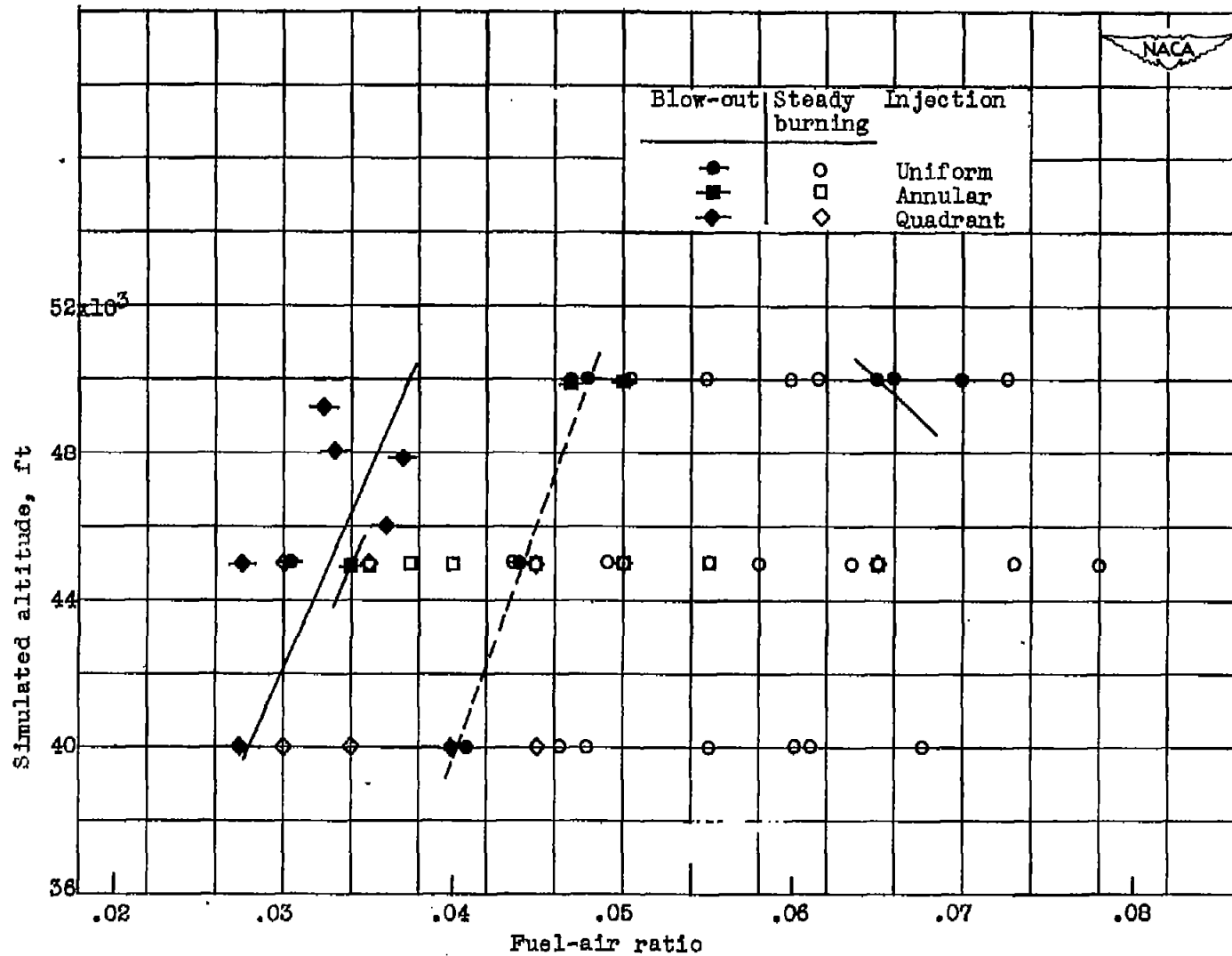
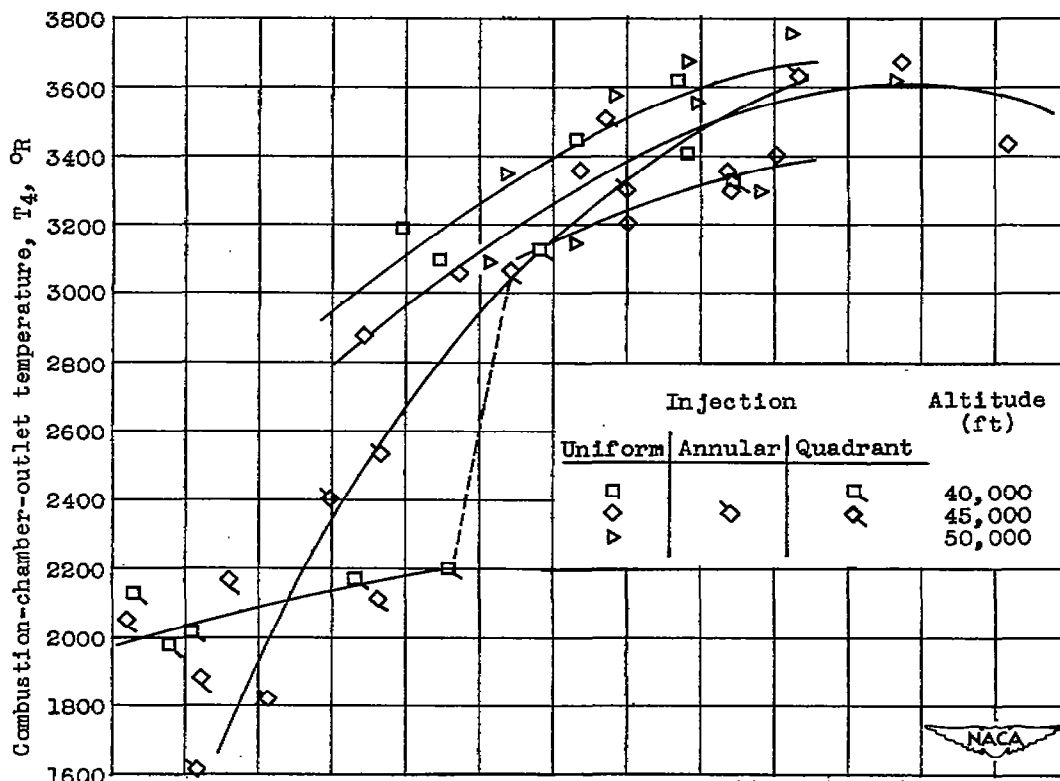
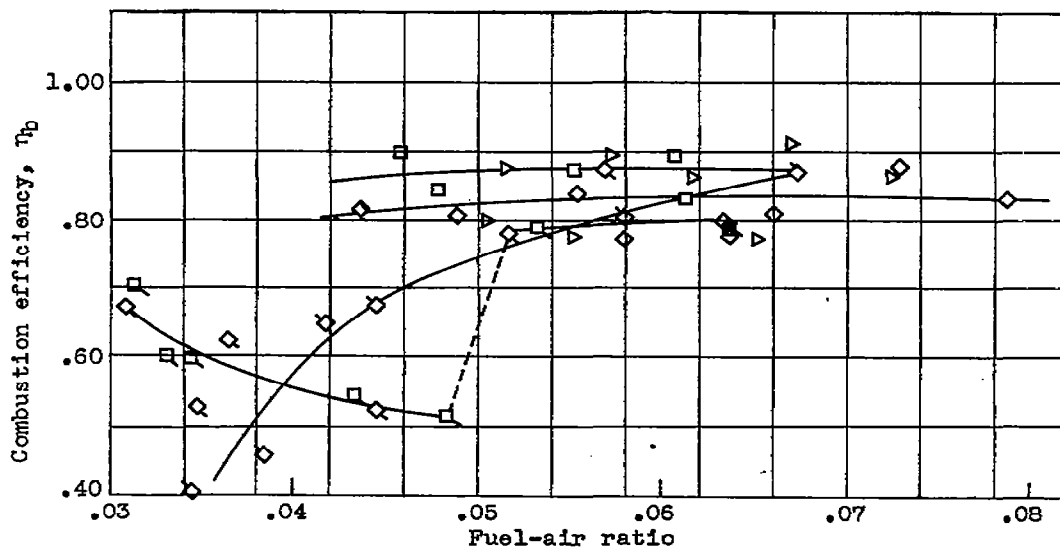


Figure 22. - Operational limits for configuration 3. Double-manifold fuel system with manifolds located at 20- and 24.6-inch diameters using variable-area, spring-loaded fuel nozzles and flame holder with 1-inch wide gutters and 55-percent blocked area.



(a) Temperature variation.



(b) Combustion-efficiency variation.

Figure 23. - Variation of combustion-chamber-outlet temperature and combustion efficiency with fuel-air ratio for configuration 3. Double-manifold fuel system with manifolds located at 20- and 24.6-inch diameters using variable-area, spring-loaded fuel nozzles and flame holder with 1-inch wide gutters and 55-percent blocked area.

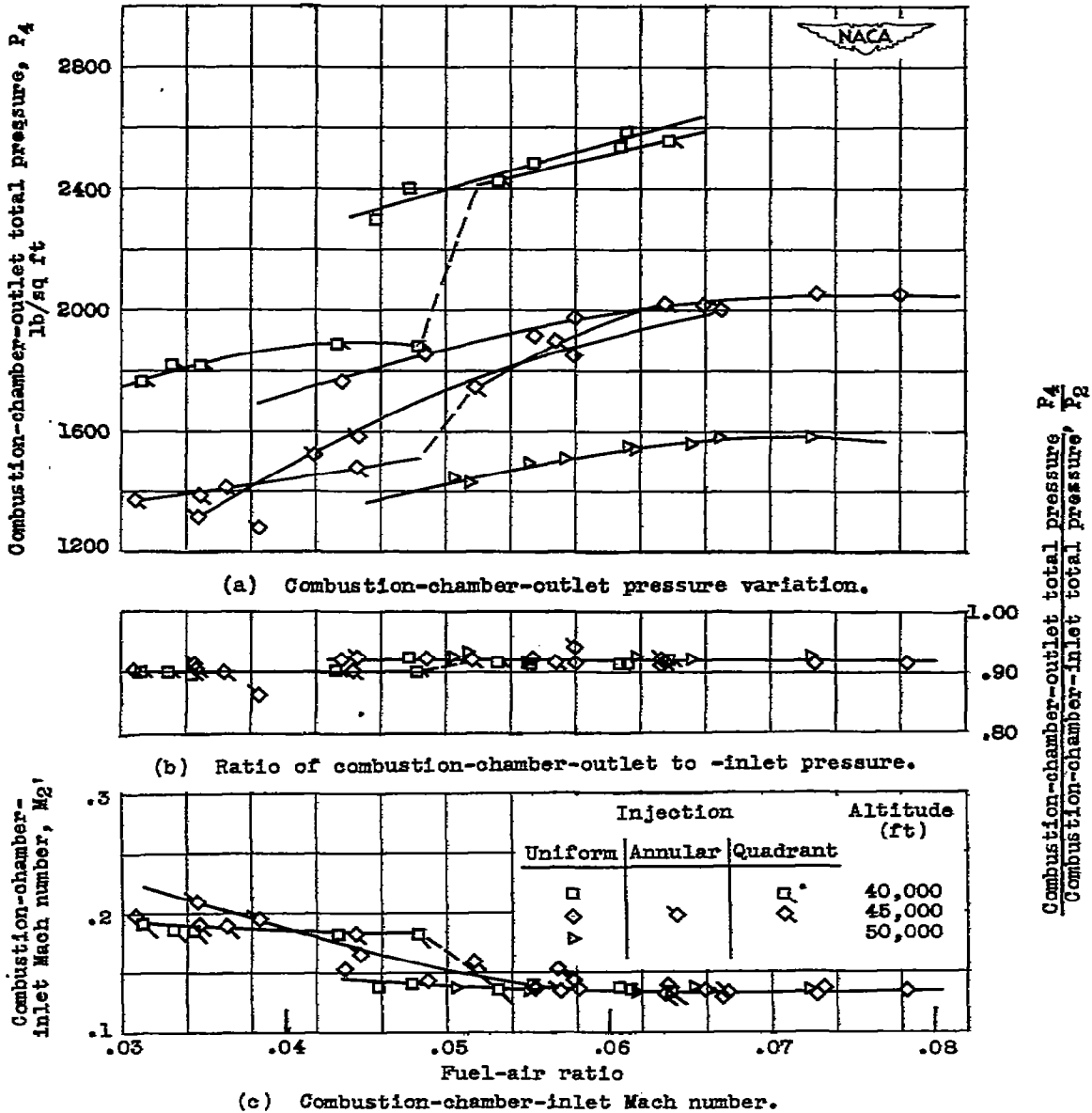


Figure 24. - Variation of engine pressures and Mach numbers with fuel-air ratio for configuration 3. Double-manifold fuel system with manifolds located at 20- and 24.6-inch diameters using variable-area, spring-loaded fuel nozzles and flame holder with 1-inch wide gutters and 55-percent blocked area.

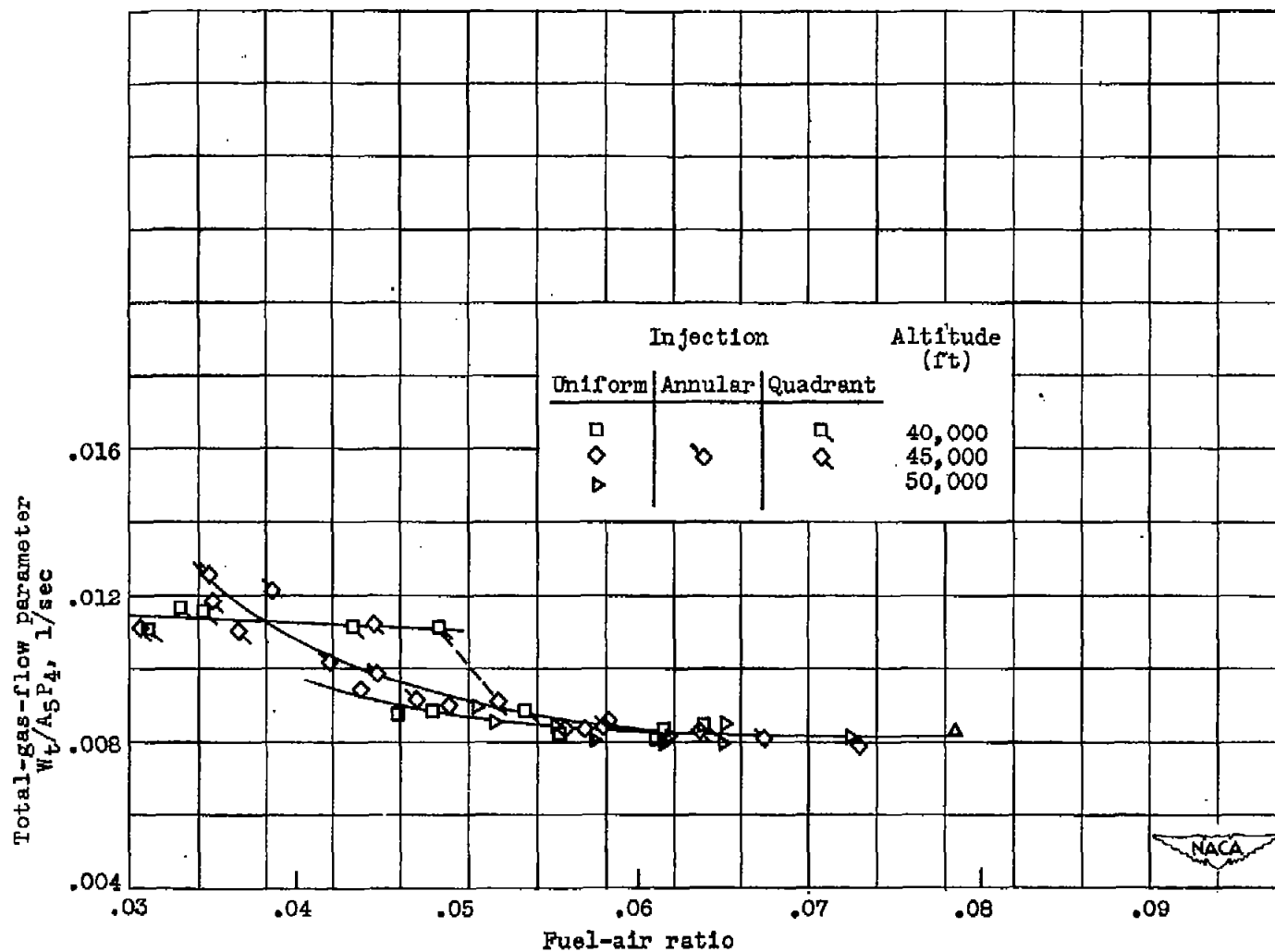


Figure 25. - Gas-flow correlation for configuration 3. Double-manifold fuel system with manifolds located at 20- and 24.6-inch diameters using variable-area, spring-loaded fuel nozzles and flame holder with 1-inch wide gutters and 55-percent blocked area.

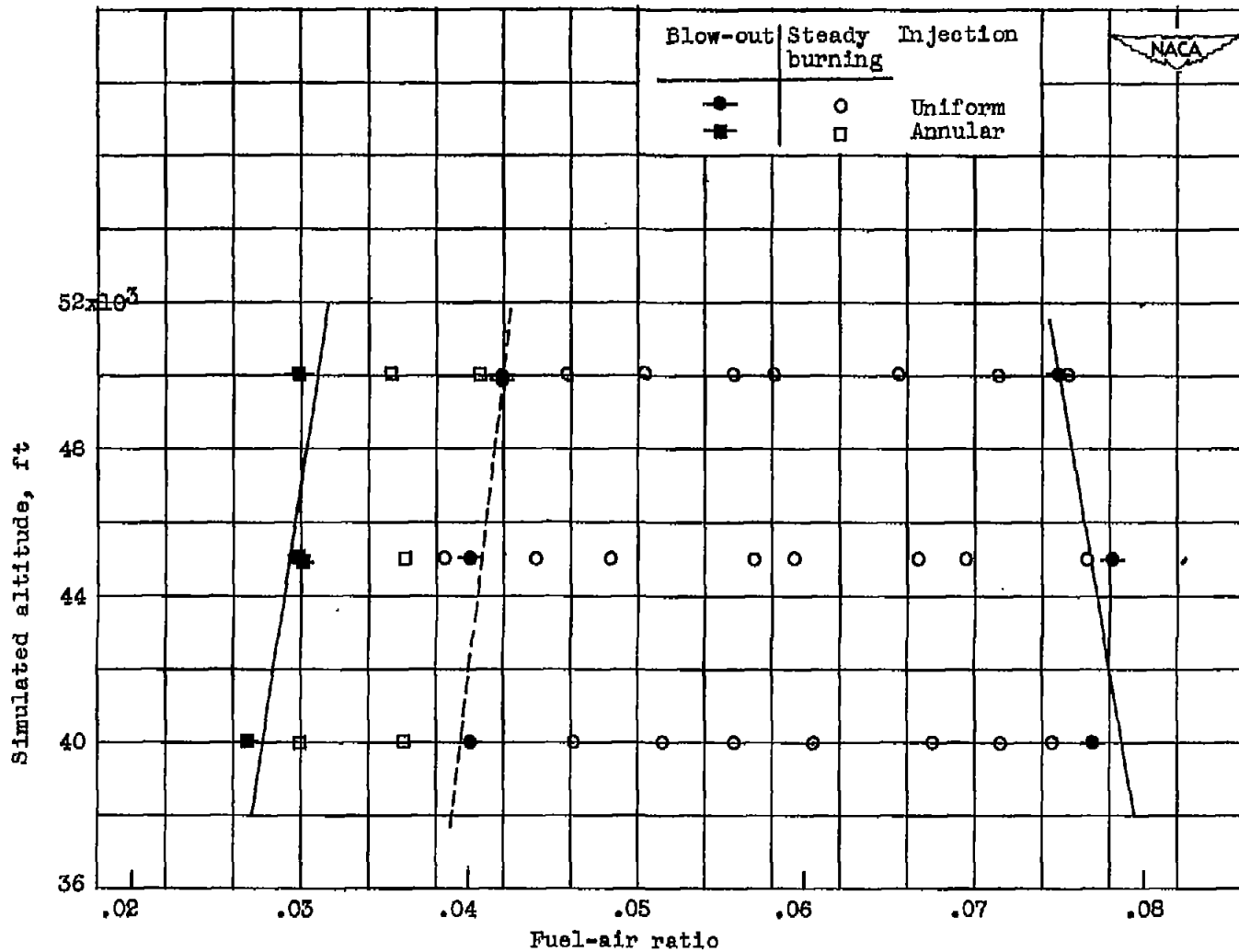
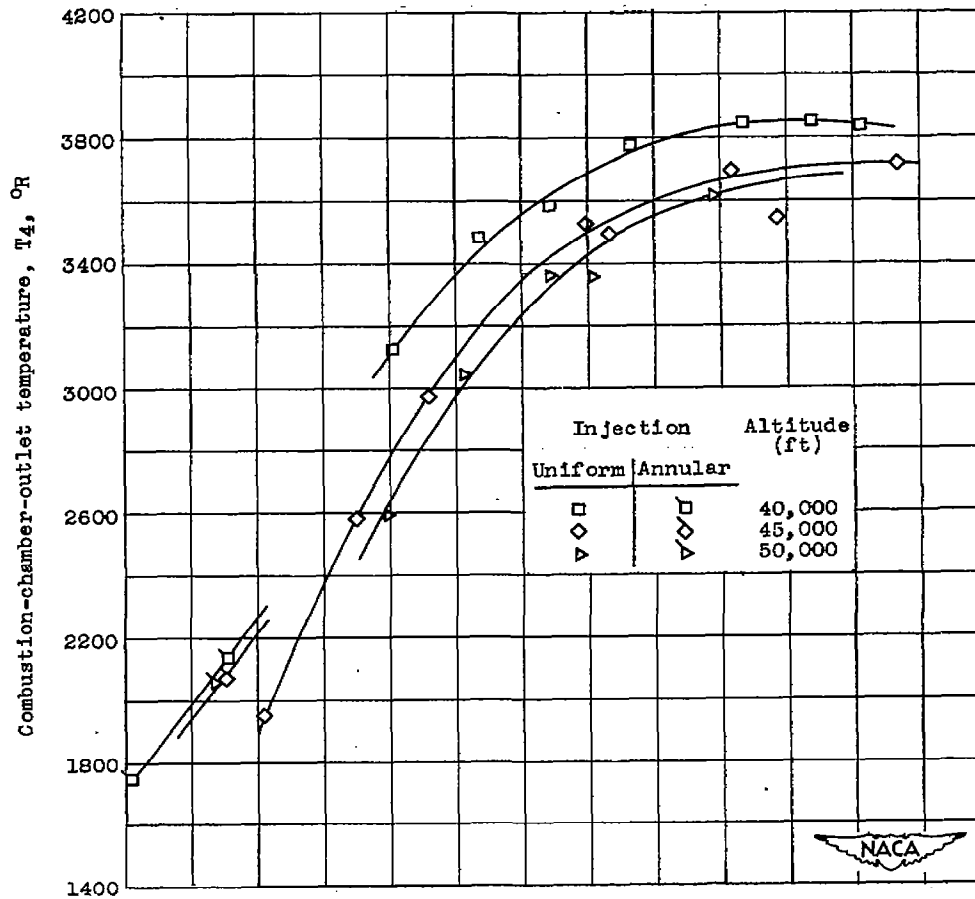
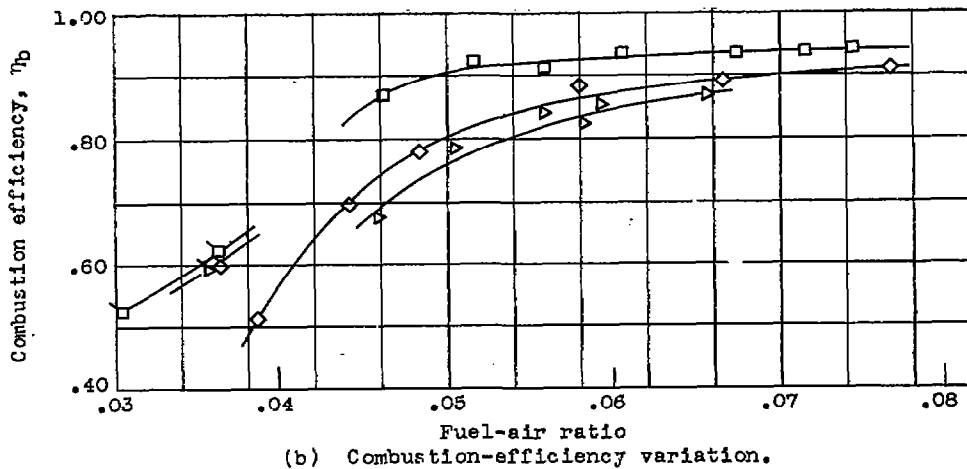


Figure 26. - Operational limits for configuration 4. Double-manifold fuel system with manifolds located at 20- and 24.6-inch diameters using variable-area, spring-loaded fuel nozzles and flame holder with 2-inch wide gutters and 45-percent blocked area.



(a) Combustion-chamber-outlet temperature variation.



(b) Combustion-efficiency variation.

Figure 27. - Variation of combustion-chamber-outlet temperature and combustion efficiency for configuration 4. Double-manifold fuel system with manifolds located at 20- and 24.6-inch diameters using variable-area, spring-loaded fuel nozzles and flame holder with 2-inch wide gutters and 45-percent blocked area.

CONFIDENTIAL

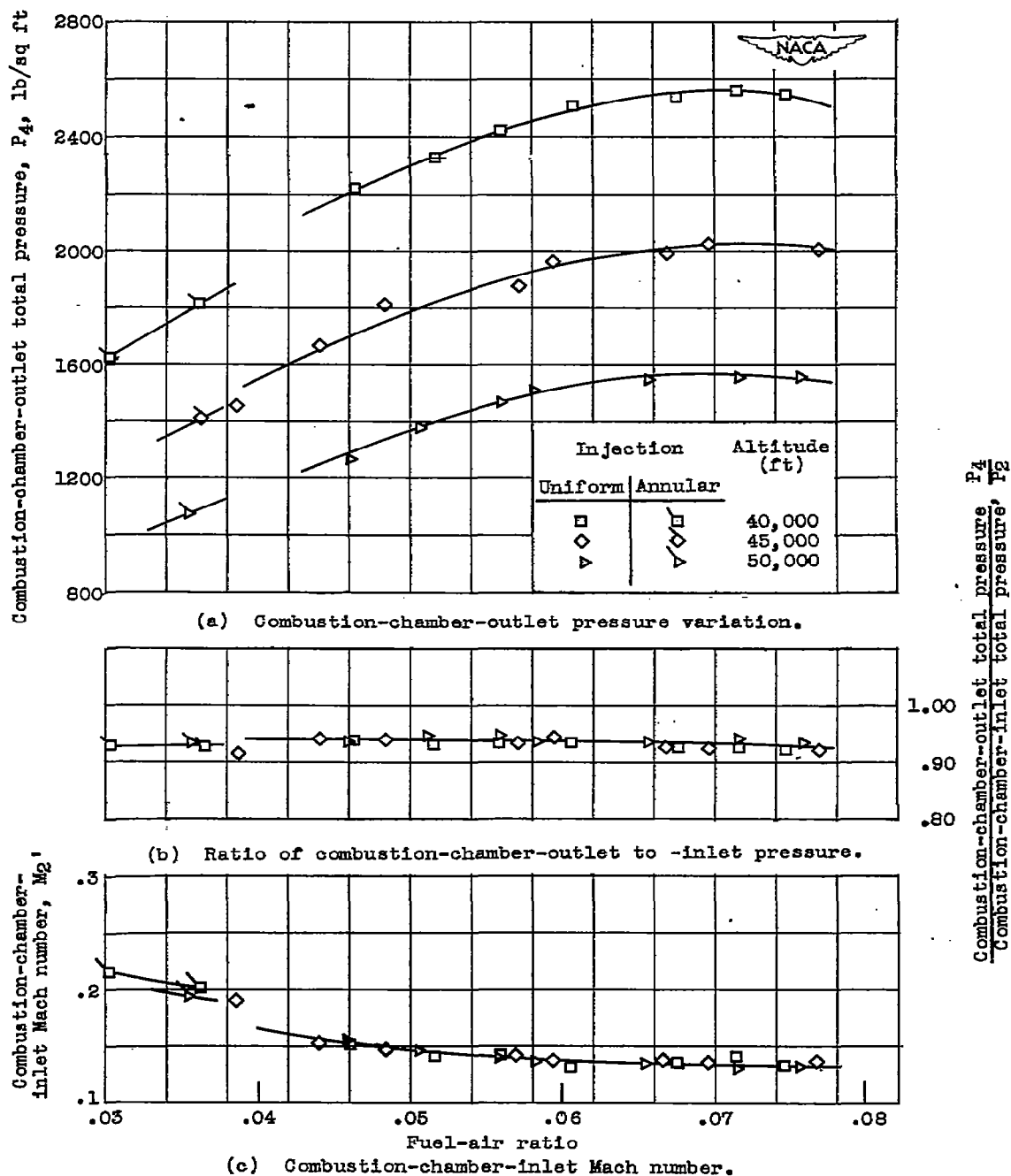


Figure 28. - Variation of engine pressures and Mach numbers with fuel-air ratio for configuration 4. Double-manifold fuel system with manifolds located at 20- and 24.6-inch diameters using variable-area, spring-loaded fuel nozzles and flame holder with 2-inch wide gutters and 45-percent blocked area.

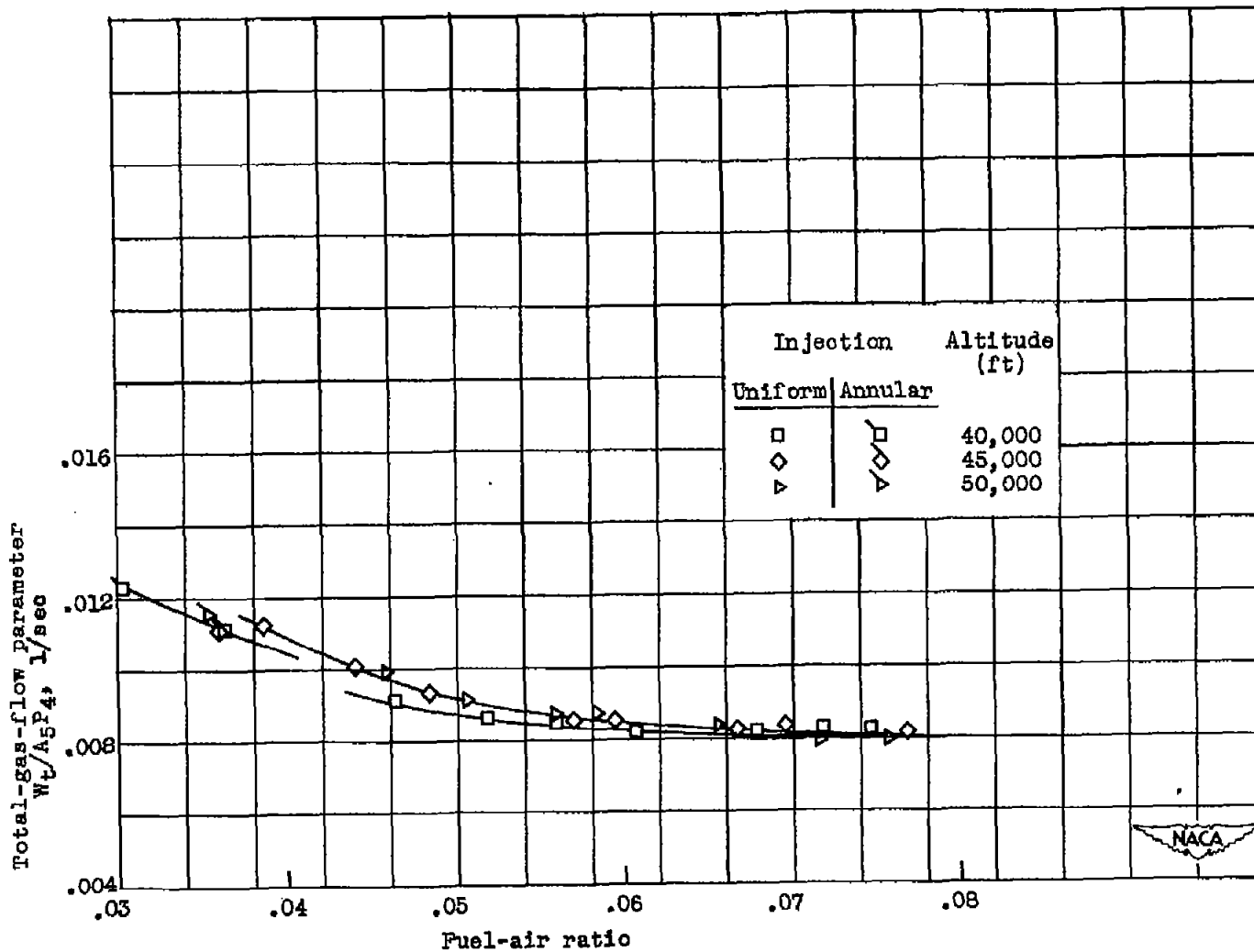
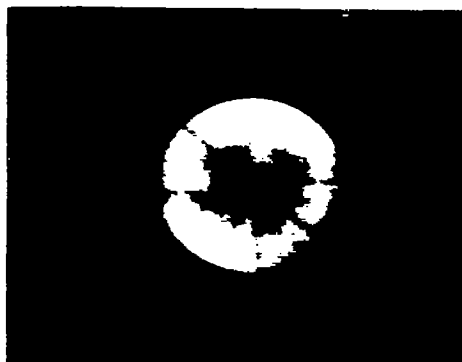


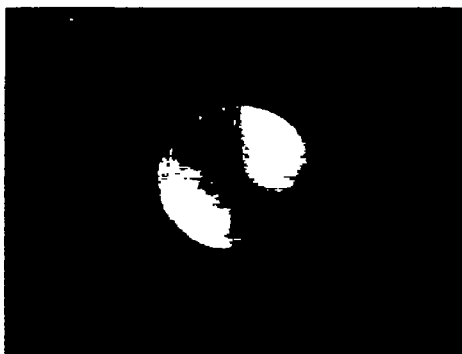
Figure 29. - Gas-flow correlation for configuration 4. Double-manifold fuel system with manifolds located at 20- and 24.6-inch diameters using variable-area, spring-loaded fuel nozzles and flame holder with 2-inch wide gutters and 45-percent blocked area.



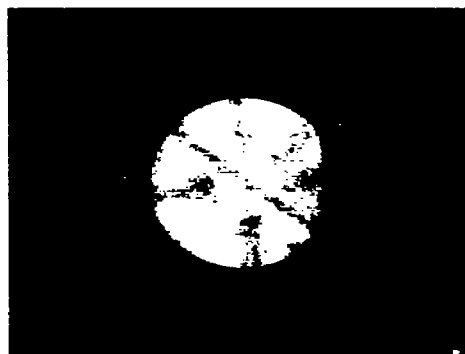
(a) Uniform injection,
configuration 1.



(b) Uniform injection,
configuration 2.



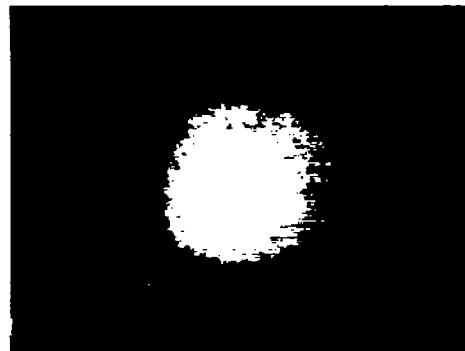
(c) Quadrant injection,
configuration 2.



(d) Uniform injection,
configuration 3.



(e) Uniform injection,
configuration 4.



(f) Annular injection,
configuration 4.

Figure 30. - Combustion photographs.



C-25451
3-20-50

NASA Technical Library



3 1176 01435 0020